

# X-ray variability of NGC 2516 stars in the XMM-Newton observations

A. Marino<sup>1</sup>, G. Micela<sup>2</sup>, I. Pillitteri<sup>1</sup>, and G. Peres<sup>1</sup>

<sup>1</sup> DSFA, Università di Palermo, Piazza del Parlamento 1, 90134 Palermo - ITALY;

<sup>2</sup> INAF - Osservatorio Astronomico di Palermo, Piazza del Parlamento 1, 90134 Palermo - ITALY;

Received 9 December 2005 / accepted 01 May 2006

**Abstract.** We present the characteristics of the X-ray variability of stars in the cluster NGC 2516 as derived from XMM-Newton/EPIC/pn data. The X-ray variations on short (hours), medium (months), and long (years) time scales have been explored. We detected 303 distinct X-ray sources by analysing six EPIC/pn observations; 194 of them are members of the cluster. Stars of all spectral types, from the early-types to the late-M dwarfs, were detected. The Kolmogorov-Smirnov test applied to the X-ray photon time series shows that, on short time scales, only a relatively small fraction (ranging from 6% to 31% for dG and dF, respectively) of the members of NGC 2516 are variable with a confidence level  $\geq 99\%$ ; however, it is possible that the fraction is small only because of the poor statistics. The time X-ray amplitude distribution functions (XAD) of a set of dF7-dK2 stars, derived on short (hours) and medium (months) time scales, seem to suggest that medium-term variations, if present, have a much smaller amplitude than those on short time scales; a similar result is also obtained for dK3-dM stars. The amplitude variations of late-type stars in NGC 2516 are consistent with those of the coeval Pleiades stars. Comparing these data with those of ROSAT/PSPC, collected 7-8 years earlier, and of ROSAT/HRI, just 4-5 years earlier, we find no evidence of significant variability on the related time scales, suggesting that long-term variations due to activity cycles similar to the solar cycle are not common among young stars. Indications of spectral variability was found in one star whose spectra at three epochs were available.

**Key words.** X-ray: stars – Stars: activity – Stars: early-type – Stars: late-type – Open clusters and associations: individual: NGC 2516

## 1. Introduction

Observations using the *Einstein* observatory, nearly 30 years ago, showed the ubiquity of stellar X-ray emission throughout the HR diagram (Vaiana et al. 1981). X-ray emission from stars has been attributed to several physical mechanisms depending on the mass of the star. Going from high to low mass, they include winds, dynamo, and turbulent dynamo. Variability studies are one of the best ways to explore these mechanisms and to infer physical conditions of the regions where X-ray emission originates and their evolution along stellar life (e.g. Montmerle et al. 1983; Ambruster et al. 1987; Stern et al. 1995; Marino et al. 2003a,b; Pillitteri et al. 2005). In this context, open clusters, providing large, chemically homogeneous, and precisely dated samples of stars, are ideal laboratories for studying coronal emitters and for constraining the X-ray-generating mechanisms. Comparative studies of the variability properties of homogeneous classes are excellent for

diagnosing and determining the origin of the X-ray emission.

In this perspective we have analysed the X-ray variability properties of homogeneous samples (with respect to mass and age): dF7-dK2 and dK3-dM stars in the solar neighbourhood, dF7-dK2, and dK3-dM of Pleiades observed with ROSAT-PSPC (Marino et al. 2000, 2002, 2003b). These studies show that the short-term variability of solar-type stars decreases with age (together with luminosity), while long-term variability increases. In contrast, the short-term variability of low mass stars is present in all stellar life phases while long-term variations have never been observed.

Also called the "Southern Pleiades", NGC 2516 is a rich and young open cluster in the constellation of Carina, that has been observed several times at the XMM-Newton observatory, thereby allowing us the study of X-ray variability properties on multiple time scales. At a distance of less than 400 pc (387 pc, Jeffries et al. 1997; 346 pc, Robichon et al. 1999), the cluster contains about 1300 known members spanning all spectral types and enabling simultaneous study of the different processes driving X-

ray emission from stars with different internal structures. The metallicity of the cluster is controversial; several photometric studies have suggested a metal underabundance by a factor of 2 with respect to the Sun (e.g. Jeffries et al. 1997, 1998, 2001; Pinsonneault et al. 1998), while Terndrup et al. (2002) have found solar-like metal abundance on the basis of high-resolution spectra. Since metallicity affects the depth of the convection zone, which in turn should influence the dynamo's efficiency, observable differences in the X-ray emission levels may be expected between solar and sub-solar abundances (Micela et al. 2000). The ROSAT observations have shown that the G and K members in NGC 2516 were underactive in X-rays with respect to the Pleiades G and K stars, while no difference was found for M stars. As discussed by Jeffries et al. (1997) and Micela et al. (2000), these results could be attributed to a low-metallicity effect, although when taking the recent optical data into account (Terndrup et al. 2002) these explanations are questioned. Also a recent analysis of summed XMM/EPIC data (Pillitteri et al. 2006) shows that late-types stars in NGC 2516 are significantly less luminous than those of the Pleiades.

NGC 2516 has been observed several times with Chandra and the analysis of the observations was made by Harnden et al. (2001) and Damiani et al. (2003). Wolk et al. (2004) used Chandra data for a timing analysis of NGC 2516 stars, finding that the stochastic variability rate is similar for all sources in their sample, while the time scale of variability is shorter for later-type stars.

In this paper we present a study of the X-ray variability of the NGC 2516 stars analysing six XMM-Newton/EPIC observations spanning  $\sim 19$  months. We explore X-ray variability properties on short (hours), medium (months), and long (years) time scales, we compare our data with those obtained for the coeval Pleiades, and we search for spectral variability.

The structure of the paper is the following: Sect. 2 describes the XMM-Newton/EPIC observation set and the data analysis; Sect. 3 and 4 present the time and the spectral analysis, respectively; Sect. 5 summarises the main results.

## 2. X-ray observations and data analysis

NGC 2516 was observed many times during the first two years of satellite calibration operations. We used only EPIC-pn data detector, since the MOS data have a lower statistic than pn. The characteristic of the six EPIC/pn observations are summarised in Table 1. The progressive letter in column 1 is a reference to Table 2. The first two observations were centred at 7:58:20, -60:52:13 (J2000) and the remaining at 119.58:22, -60:45:36 (J2000). All six observations that we consider were performed with the thick filter. The data span 19 months with exposure time ranging from 6 ks to  $\sim 22$  ks. All pn data were processed using the XMM-Newton Science Analysis System (SAS) 6.0.0. We used the *epchain* task to process the EPIC/pn observation data file, obtaining six lists with time, posi-

tion, and energy of the events recorded in the pn detector. To minimise the background due to non-X-ray events, we retained only single, double, triple, and quadruple pixel events in the 0.3-5.5 keV band. We limited the energy band to 0.3-5.5 keV, since data below 0.3 keV are contaminated by low-energy electronic noise events, while background counts dominate above 5.5 keV for coronal sources (e.g. Read & Ponman 2003). Furthermore, we filtered the data to maximise the signal-to-noise ratio and to minimise the so-called proton flare phenomenon, which produces an enhancement of noise due to protons "focused" by XMM-Newton mirrors and essentially indistinguishable from bona-fide X-ray events. To this end we applied a technique developed at INAF - Osservatorio Astronomico of Palermo (Sciortino et al. 2002) that maximises the statistical significance of weak sources by identifying and removing fractions of the exposure time strongly affected by high-background episodes.

### 2.1. Source detection

Source detection and X-ray photometry were obtained in the 0.3 - 5.5 keV bandpass using the wavelet detection code developed at the INAF- Osservatorio Astronomico di Palermo and based on the algorithm previously developed for the ROSAT/PSPC (Damiani et al. 1997a,b) and adapted to the XMM-Newton case. Large sets of simulations of pure background signal were performed to derive the appropriate detection threshold that limits the number of spurious detections. We adopted a threshold that statistically retains only one spurious source per field. An exposure map for each observation was created with the SAS task *eexpmap* to perform this analysis. For each of the six observations, we have found a number of X-ray sources ranging from 95 (Obs. e in Table 1) to 184 (Obs. c in Table 1). In order to find the X-ray multiply observed sources, we cross-matched the detections of each observation with all the others adopting a threshold of  $20''$ , derived by taking the formal error of the detected source positions into account. However we found that more than 90% of the cross-matchs are within  $8''$ . We also found that 42 sources were detected six times, 23 five times, 39 four time, 40 three times, 60 two times, and 99 just one.

### 2.2. Cluster members and identifications

We compiled an optical catalog of cluster members based on the list of 1254 stars compiled by Jeffries et al. (2001) and based on B, V, and I photometry. Furthermore we appended 43 cluster stars brighter than  $V=9.8$  that were not present in the former sample. The number of X-ray sources identified as optical members are reported in column 7 of Table 1 for each of the six observations; the number of the optical members in each observation is reported in column 8. The cross-identification between X-ray and optical sources for each of the six observations was made in two steps: in the first we searched for a systematic offset

**Table 1.** XMM-Newton/EPIC/pn observations of NGC 2516

Obs.	Obs. Id	Orbit Nr.	Filtered Time [ks]	Start Date	Nr. of X-ray sources	Nr. of detected members	Nr. of optical members
<i>a</i>	0113891001	060	19.8	2000 April 06	128	87	409
<i>b</i>	0113891101	060	14.3	2000 April 07	118	73	408
<i>c</i>	0126511201	092	22.3	2000 June 10	184	128	419
<i>d</i>	0134531201	209	18.8	2001 January 29	174	121	408
<i>e</i>	0134531301	209	6.0	2001 January 29	95	68	402
<i>f</i>	0134531501	346	18.5	2001 October 29	168	112	423

**Table 2.** X-ray and optical properties of NGC 2516 members in the XMM-Newton/EPIC/pn observations having more than 25 counts.

JTH	Obs.	Ra J2000	Dec J2000	V	B-V	V-I	Exposure [sec]	Rate $\pm$ err cnt/ks	Results of the K-S test
323	<i>f</i>	07:56:22.80	-60:51:42.7	11.556	0.513	0.659	4894.6	16.750 $\pm$ 1.850	-
15496	<i>a</i>	07:56:46.30	-60:48:59.5	8.360	0.020		8094.8	4.200 $\pm$ 0.720	-
15496	<i>b</i>	07:56:46.30	-60:48:59.5	8.360	0.020		5880.3	5.100 $\pm$ 0.931	-
15496	<i>c</i>	07:56:46.30	-60:48:59.5	8.360	0.020		8806.8	4.825 $\pm$ 0.740	-
15496	<i>d</i>	07:56:46.30	-60:48:59.5	8.360	0.020		6764.2	5.915 $\pm$ 0.935	90%- 99%
15496	<i>f</i>	07:56:46.30	-60:48:59.5	8.360	0.020		6030.5	5.305 $\pm$ 0.938	-
15497	<i>a</i>	07:56:46.30	-60:48:59.5	8.780	0.090		8094.8	4.200 $\pm$ 0.720	-
15497	<i>b</i>	07:56:46.30	-60:48:59.5	8.780	0.090		5880.3	5.100 $\pm$ 0.931	-
15497	<i>c</i>	07:56:46.30	-60:48:59.5	8.780	0.090		8806.8	4.825 $\pm$ 0.740	-
15497	<i>d</i>	07:56:46.30	-60:48:59.5	8.780	0.090		6764.2	5.915 $\pm$ 0.935	90%-99%
15497	<i>f</i>	07:56:46.30	-60:48:59.5	8.780	0.090		6030.5	5.305 $\pm$ 0.938	-
397	<i>c</i>	07:56:47.16	-60:43:22.1	16.324	1.331	1.655	9381.9	7.460 $\pm$ 0.890	-
397	<i>d</i>	07:56:47.16	-60:43:22.1	16.324	1.331	1.655	6619.6	5.890 $\pm$ 0.940	-
397	<i>f</i>	07:56:47.16	-60:43:22.1	16.324	1.331	1.655	6596.5	7.280 $\pm$ 1.050	$\geq$ 99%
400	<i>f</i>	07:56:47.88	-60:56:48.5	10.854	0.344	0.452	4894.6	15.940 $\pm$ 1.800	-
402	<i>a</i>	07:56:48.00	-60:51: 9.5	18.353	1.640	2.376	8729.1	3.090 $\pm$ 0.600	-
401	<i>c</i>	07:56:48.26	-60:46:33.9	15.410	1.268	1.545	9572.7	12.430 $\pm$ 1.140	-
401	<i>d</i>	07:56:48.26	-60:46:33.9	15.410	1.268	1.545	7087.5	8.180 $\pm$ 1.070	-
401	<i>a</i>	07:56:48.26	-60:46:33.9	15.410	1.268	1.545	7313.0	7.250 $\pm$ 1.000	-
401	<i>b</i>	07:56:48.26	-60:46:33.9	15.410	1.268	1.545	5323.5	6.760 $\pm$ 1.130	-
401	<i>e</i>	07:56:48.26	-60:46:33.9	15.410	1.268	1.545	2246.7	11.130 $\pm$ 2.230	-
420	<i>c</i>	07:56:54.36	-60:47:22.1	17.287	1.561	2.147	10091.0	3.570 $\pm$ 0.590	-
424	<i>b</i>	07:56:55.01	-60:58:11.5	17.316	1.511	2.006	5969.2	6.370 $\pm$ 1.030	-
432	<i>c</i>	07:56:59.62	-60:47: 1.3	9.698	0.146	0.198	10757.0	4.740 $\pm$ 0.660	$\geq$ 99%
432	<i>f</i>	07:56:59.62	-60:47: 1.3	9.698	0.146	0.198	7493.5	3.870 $\pm$ 0.720	-
432	<i>a</i>	07:56:59.62	-60:47: 1.3	9.698	0.146	0.198	8514.1	4.820 $\pm$ 0.750	$\geq$ 99%
468	<i>c</i>	07:57:10.20	-60:48: 1.5	12.437	0.602	0.718	11899.0	5.130 $\pm$ 0.660	-
469	<i>d</i>	07:57:10.37	-60:44:10.6	13.330		0.839	8868.1	1.520 $\pm$ 0.414	-
474	<i>d</i>	07:57:10.37	-60:44:10.6	13.289	0.732	0.843	8868.1	1.520 $\pm$ 0.414	-
483	<i>c</i>	07:57:10.92	-60:49: 7	18.397	1.499	2.371	11433.0	5.860 $\pm$ 0.720	$\geq$ 99%
478	<i>c</i>	07:57:11.04	-60:39:36.3	13.852	0.891	0.995	10559.0	1.375 $\pm$ 0.361	90%-99%
478	<i>d</i>	07:57:11.04	-60:39:36.3	13.852	0.891	0.995	7272.0	1.995 $\pm$ 0.524	90%-99%
481	<i>c</i>	07:57:11.04	-60:39:36.3	13.661	0.874	0.987	10559.0	1.375 $\pm$ 0.361	90%-99%
481	<i>d</i>	07:57:11.04	-60:39:36.3	13.661	0.874	0.987	7272.0	1.995 $\pm$ 0.524	90%-99%
490	<i>d</i>	07:57:12.77	-60:33: 7.3	14.576	1.015	1.080	4950.0	15.350 $\pm$ 1.760	-
490	<i>f</i>	07:57:12.77	-60:33: 7.3	14.576	1.015	1.080	4984.5	10.430 $\pm$ 1.450	-
492	<i>a</i>	07:57:12.89	-60:45: 2.8	20.212		2.968	8460.7	5.080 $\pm$ 0.780	-
496	<i>c</i>	07:57:14.23	-60:40: 53	12.240	0.674	0.769	11740.0	8.690 $\pm$ 0.860	-
496	<i>d</i>	07:57:14.23	-60:40: 53	12.240	0.674	0.769	8122.4	21.670 $\pm$ 1.630	$\geq$ 99%
496	<i>f</i>	07:57:14.23	-60:40: 53	12.240	0.674	0.769	8409.0	12.010 $\pm$ 1.200	-
496	<i>a</i>	07:57:14.23	-60:40: 53	12.240	0.674	0.769	5799.7	9.830 $\pm$ 1.300	-
496	<i>b</i>	07:57:14.23	-60:40: 53	12.240	0.674	0.769	4391.7	12.070 $\pm$ 1.660	-
496	<i>e</i>	07:57:14.23	-60:40: 53	12.240	0.674	0.769	2550.9	14.110 $\pm$ 2.350	-
501	<i>c</i>	07:57:15.48	-60:38:55.3	15.035	1.068	1.200	10636.0	3.760 $\pm$ 0.590	-
501	<i>d</i>	07:57:15.48	-60:38:55.3	15.035	1.068	1.200	7268.2	4.400 $\pm$ 0.780	-
506	<i>c</i>	07:57:16.68	-60:47:12.7	12.035	0.537	0.652	13034.0	4.140 $\pm$ 0.560	$\geq$ 99%
15499	<i>c</i>	07:57:19.66	-60:48:43.3	9.290		0.120	12773.0	5.950 $\pm$ 0.680	-
15499	<i>d</i>	07:57:19.66	-60:48:43.3	9.290		0.120	10110.0	9.300 $\pm$ 0.960	-
15499	<i>f</i>	07:57:19.66	-60:48:43.3	9.290		0.120	9012.1	6.660 $\pm$ 0.860	-
15499	<i>a</i>	07:57:19.66	-60:48:43.3	9.290		0.120	10944.0	7.950 $\pm$ 0.850	-
15499	<i>b</i>	07:57:19.66	-60:48:43.3	9.290		0.120	8154.9	4.170 $\pm$ 0.720	-
522	<i>c</i>	07:57:20.62	-60:55:46.4	17.301	1.476	2.020	7939.8	5.670 $\pm$ 0.840	-

between X-ray source positions and the optical position of the members. In the second, we corrected the X-ray positions for this systematic offset, before matching the X-ray and optical member positions, and then retained an identification if the offset between X-ray and optical positions

was less than 8''. The choice of such a limiting distance is a good compromise between the attempt to minimise the number of spurious identifications for an offset bona-fide optical counterparts. For 8 cases it was impossible to resolve very close stars, owing to the limited spatial resolution.

**Table 2.** Continued

JTH	Obs.	Ra <sub>optt</sub> J2000	Dec <sub>optt</sub> J2000	V	B-V	V-I	Exposure [sec]	Rate ± err cnt/ks	K-S
522	e	07:57:20.62	-60:55:46.4	17.301	1.476	2.020	2240.6	11.160 ± 2.230	-
523	c	07:57:20.86	-60:44: 0.8	14.945	1.065	1.204	13991.0	3.790 ± 0.520	-
523	d	07:57:20.86	-60:44: 0.8	14.945	1.065	1.204	10000.0	7.200 ± 0.850	-
523	f	07:57:20.86	-60:44: 0.8	14.945	1.065	1.204	9982.4	6.410 ± 0.800	-
523	a	07:57:20.86	-60:44: 0.8	14.945	1.065	1.204	8317.3	7.570 ± 0.950	≥99%
523	b	07:57:20.86	-60:44: 0.8	14.945	1.065	1.204	6039.3	6.460 ± 1.030	-
530	c	07:57:23.23	-60:49:39.8	11.320	0.517	0.659	12691.0	3.780 ± 0.550	-
530	d	07:57:23.23	-60:49:39.8	11.320	0.517	0.659	10283.0	6.710 ± 0.810	-
530	f	07:57:23.23	-60:49:39.8	11.320	0.517	0.659	9046.0	3.100 ± 0.580	-
530	a	07:57:23.23	-60:49:39.8	11.320	0.517	0.659	12319.0	6.010 ± 0.700	-
530	b	07:57:23.23	-60:49:39.8	11.320	0.517	0.659	8979.4	4.900 ± 0.740	-
539	c	07:57:25.13	-60:46:51.5	13.047	0.684	0.794	14454.0	2.970 ± 0.450	-
540	f	07:57:25.44	-60:56:51.6	15.064	1.260	1.413	5685.5	4.920 ± 0.930	-
542	c	07:57:26.09	-60:45:40.4	15.935	1.288	1.495	14839.0	4.040 ± 0.520	-
542	a	07:57:26.09	-60:45:40.4	15.935	1.288	1.495	9730.6	4.730 ± 0.700	-
542	b	07:57:26.09	-60:45:40.4	15.935	1.288	1.495	7078.9	4.240 ± 0.770	-
547	c	07:57:28.39	-60:51:26.6	13.399	0.742	0.873	11805.0	6.440 ± 0.740	-
547	d	07:57:28.39	-60:51:26.6	13.399	0.742	0.873	10051.0	5.470 ± 0.740	-
547	f	07:57:28.39	-60:51:26.6	13.399	0.742	0.873	8577.4	4.430 ± 0.720	-
547	a	07:57:28.39	-60:51:26.6	13.399	0.742	0.873	13686.0	2.850 ± 0.460	90%-99%
547	b	07:57:28.39	-60:51:26.6	13.399	0.742	0.873	9920.6	5.440 ± 0.740	-
551	f	07:57:29.30	-60:46: 6.6	18.142	1.637	2.357	10542.0	3.040 ± 0.540	-
552	c	07:57:29.57	-60:50:12.8	13.643	0.812	0.960	12995.0	2.540 ± 0.440	-
552	d	07:57:29.57	-60:50:12.8	13.643	0.812	0.960	10666.0	4.310 ± 0.640	-
552	f	07:57:29.57	-60:50:12.8	13.643	0.812	0.960	9385.2	20.780 ± 1.490	≥99%
553	d	07:57:30.58	-60:52:26.0	19.088	2.748		9400.1	5.430 ± 0.760	90%-99%
553	f	07:57:30.58	-60:52:26.0	19.088	2.748		8331.1	19.090 ± 1.510	-
553	a	07:57:30.58	-60:52:26.0	19.088	2.748		13444.0	4.090 ± 0.550	-
553	b	07:57:30.58	-60:52:26.0	19.088	2.748		9549.9	3.350 ± 0.590	-
557	c	07:57:30.96	-60:38:27.1	18.058	1.661	2.183	11740.0	4.940 ± 0.650	-
556	c	07:57:30.98	-60:48:33.1	14.037	0.817	0.979	14460.0	10.930 ± 0.870	-
556	d	07:57:30.98	-60:48:33.1	14.037	0.817	0.979	11513.0	13.200 ± 1.070	90%-99%
556	f	07:57:30.98	-60:48:33.1	14.037	0.817	0.979	10313.0	15.220 ± 1.210	-
556	a	07:57:30.98	-60:48:33.1	14.037	0.817	0.979	12444.0	5.300 ± 0.650	90%-99%
556	b	07:57:30.98	-60:48:33.1	14.037	0.817	0.979	8995.5	8.120 ± 0.950	-
556	e	07:57:30.98	-60:48:33.1	14.037	0.817	0.979	3658.3	9.020 ± 1.570	-
562	a	07:57:31.46	-60:59:31.0	10.899	0.329		10338.0	14.030 ± 1.160	-
562	b	07:57:31.46	-60:59:31.0	10.899	0.329		7540.9	15.380 ± 1.430	-
570	d	07:57:33.89	-60:50:43.7	18.731	1.600	2.436	10971.0	2.550 ± 0.480	-
576	c	07:57:36.29	-60:48:14.7	13.730	0.809	0.907	15331.0	2.020 ± 0.360	-
15500	c	07:57:37.82	-60:54:35.8	8.810	0.060		9793.7	7.960 ± 0.900	-
15500	d	07:57:37.82	-60:54:35.8	8.810	0.060		8852.9	8.360 ± 0.970	-
15500	f	07:57:37.82	-60:54:35.8	8.810	0.060		7481.0	4.010 ± 0.730	-
15500	a	07:57:37.82	-60:54:35.8	8.810	0.060		14338.0	7.670 ± 0.730	-
15500	b	07:57:37.82	-60:54:35.8	8.810	0.060		10429.0	7.000 ± 0.820	-
589	a	07:57:38.86	-61:02: 8.9	12.759	0.649	0.778	8670.4	9.460 ± 1.040	-
589	b	07:57:38.86	-61:02: 8.9	12.759	0.649	0.778	6300.2	8.730 ± 1.180	-
592	d	07:57:39.89	-60:46:40.1	15.707	1.337	1.598	12865.0	2.570 ± 0.450	≥99%
592	f	07:57:39.89	-60:46:40.1	15.707	1.337	1.598	11959.0	2.590 ± 0.470	-
592	a	07:57:39.89	-60:46:40.1	15.707	1.337	1.598	11461.0	3.320 ± 0.540	90%-99%
592	e	07:57:39.89	-60:46:40.1	15.707	1.337	1.598	4091.7	6.600 ± 1.270	-
600	a	07:57:40.85	-60:52:33.4	20.218	3.263		15058.0	3.250 ± 0.460	-
601	c	07:57:42.70	-60:44:21.9	12.682	0.636	0.750	17086.0	3.340 ± 0.440	-
601	d	07:57:42.70	-60:44:21.9	12.682	0.636	0.750	12818.0	3.280 ± 0.510	-
601	f	07:57:42.70	-60:44:21.9	12.682	0.636	0.750	12784.0	2.740 ± 0.460	-
603	d	07:57:43.51	-60:45: 7.8	19.565	2.643		13078.0	2.140 ± 0.400	90%-99%
615	c	07:57:47.33	-60:51:38.7	16.417	1.408	1.633	13153.0	2.810 ± 0.460	-

tion of the X-ray telescope. For these unresolved sources, the X-ray flux was divided evenly between the optical candidates in the absence of more information.

Following Damiani et al. (2003), we attribute spectral types that use B-V and V-I optical colours corrected for the average cluster reddening  $E(B-V) = 0.12$ . Detected members cover the whole mass range present in the optical catalog. Among these stars we considered in the following variability studies all those sources with more than 25 total counts in a single pn observation, for a total of 474 detections. Table 2 summarise their optical and X-ray characteristics.

### 3. Time variability

The analysis of all observations of NGC 2516 allow us to explore the X-ray variability on time scales that range from hours to 19 months. We obtained light curves in the 0.3-5.5 keV band for all detected X-ray sources by extracting the photon arrival time within circular regions selected interactively using Astronomical Data Visualization DS9 display software and subtracted from an area-scaled background. We adopted a radius of 3.5 times the radius determined by the PWADetect algorithm to select sources and background regions. In some cases we used a smaller radius to exclude contributions from nearby stars. In general, detections have relatively low statistics with 90% of

**Table 2.** Continued

JTH	Obs.	Ra <sub>ott</sub> J2000	Dec <sub>ott</sub> J2000	V	B-V	V-I	Exposure [sec]	Rate ± err cnt/ks	K-S
15501	c	07:57:47.69	-60:36:35.6	8.390	-0.010		11316.0	6.800 ± 0.780	-
15501	f	07:57:47.69	-60:36:35.6	8.390	-0.010		8449.1	6.860 ± 0.900	-
625	c	07:57:51.22	-60:42:11.9	17.771	1.589	2.120	17025.0	2.640 ± 0.390	-
624	c	07:57:51.50	-60:43:17.0	18.702		2.568	17728.0	6.710 ± 0.620	90%-99%
624	f	07:57:51.50	-60:43:17.0	18.702		2.568	13414.0	5.220 ± 0.620	-
635	f	07:57:53.38	-60:46:13.9	19.713		2.866	13631.0	6.900 ± 0.710	≥99%
635	b	07:57:53.38	-60:46:13.9	19.713		2.866	8245.2	3.880 ± 0.690	-
638	c	07:57:53.95	-60:45: 6.0	13.806	0.837	0.921	17296.0	3.580 ± 0.460	-
638	d	07:57:53.95	-60:45: 6.0	13.806	0.837	0.921	14281.0	4.200 ± 0.540	-
638	a	07:57:53.95	-60:45: 6.0	13.806	0.837	0.921	10633.0	2.450 ± 0.480	90%-99%
643	c	07:57:55.34	-60:40:41.3	12.632	0.602	0.699	16018.0	3.000 ± 0.430	-
643	d	07:57:55.34	-60:40:41.3	12.632	0.602	0.699	11282.0	4.430 ± 0.630	-
643	f	07:57:55.34	-60:40:41.3	12.632	0.602	0.699	12310.0	3.740 ± 0.550	-
643	a	07:57:55.34	-60:40:41.3	12.632	0.602	0.699	7055.0	5.390 ± 0.870	≥99%
642	c	07:57:55.44	-60:43:22.3	13.990	0.885	0.996	18167.0	2.370 ± 0.360	-
640	c	07:57:55.46	-60:48:30.0	12.905	0.719	0.876	17024.0	12.390 ± 0.850	-
640	d	07:57:55.46	-60:48:30.0	12.905	0.719	0.876	14339.0	13.180 ± 0.960	-
640	f	07:57:55.46	-60:48:30.0	12.905	0.719	0.876	13090.0	10.700 ± 0.900	90%-99%
640	a	07:57:55.46	-60:48:30.0	12.905	0.719	0.876	13504.0	4.890 ± 0.600	-
640	e	07:57:55.46	-60:48:30.0	12.905	0.719	0.876	4554.0	18.880 ± 2.040	-
647	f	07:57:56.11	-60:55: 0.2	14.322	0.935	1.008	8104.4	3.700 ± 0.680	-
647	a	07:57:56.11	-60:55: 0.2	14.322	0.935	1.008	15794.0	2.340 ± 0.390	90%-99%
647	b	07:57:56.11	-60:55: 0.2	14.322	0.935	1.008	11487.0	3.400 ± 0.540	-
652	c	07:57:57.79	-60:44:15.9	9.893	0.195	0.251	18668.0	7.550 ± 0.640	90%-99%
652	d	07:57:57.79	-60:44:15.9	9.893	0.195	0.251	14167.0	6.990 ± 0.700	-
652	f	07:57:57.79	-60:44:15.9	9.893	0.195	0.251	14365.0	7.660 ± 0.730	-
652	b	07:57:57.79	-60:44:15.9	9.893	0.195	0.251	7270.6	11.000 ± 1.230	-
652	e	07:57:57.79	-60:44:15.9	9.893	0.195	0.251	4485.8	8.250 ± 1.360	-
653	c	07:57:57.79	-60:53:40.2	14.429	0.928	1.052	11528.0	9.800 ± 0.920	90%-99%
653	d	07:57:57.79	-60:53:40.2	14.429	0.928	1.052	10778.0	8.910 ± 0.910	-
653	f	07:57:57.79	-60:53:40.2	14.429	0.928	1.052	9043.8	11.720 ± 1.140	-
653	a	07:57:57.79	-60:53:40.2	14.429	0.928	1.052	16356.0	9.170 ± 0.750	-
653	b	07:57:57.79	-60:53:40.2	14.429	0.928	1.052	11976.0	7.260 ± 0.780	-
653	e	07:57:57.79	-60:53:40.2	14.429	0.928	1.052	3419.1	10.820 ± 1.780	-
655	c	07:57:58.39	-60:45:45.5	15.153	1.279	1.420	18879.0	3.810 ± 0.450	-
661	c	07:57:59.62	-60:56:55.9	12.647	0.655	0.802	8460.4	17.140 ± 1.420	-
661	d	07:57:59.62	-60:56:55.9	12.647	0.655	0.802	8105.8	3.080 ± 0.620	-
661	f	07:57:59.62	-60:56:55.9	12.647	0.655	0.802	6791.9	9.280 ± 1.170	-
661	a	07:57:59.62	-60:56:55.9	12.647	0.655	0.802	14429.0	10.950 ± 0.870	-
661	b	07:57:59.62	-60:56:55.9	12.647	0.655	0.802	10515.0	36.900 ± 1.870	≥99%
664	c	07:58: 0.36	-60:52:12.0	15.761	1.417	1.706	13249.0	16.610 ± 1.120	≥99%
664	d	07:58: 0.36	-60:52:12.0	15.761	1.417	1.706	12333.0	7.460 ± 0.780	90%-99%
664	f	07:58: 0.36	-60:52:12.0	15.761	1.417	1.706	10544.0	5.030 ± 0.690	-
664	a	07:58: 0.36	-60:52:12.0	15.761	1.417	1.706	16123.0	5.270 ± 0.570	90%-99%
664	b	07:58: 0.36	-60:52:12.0	15.761	1.417	1.706	12094.0	3.390 ± 0.530	-
671	c	07:58: 2.28	-60:46:47.5	12.068	0.603	0.741	18785.0	17.730 ± 0.970	-
671	d	07:58: 2.28	-60:46:47.5	12.068	0.603	0.741	15374.0	18.280 ± 1.090	90%-99%
671	f	07:58: 2.28	-60:46:47.5	12.068	0.603	0.741	13863.0	14.930 ± 1.040	-
671	a	07:58: 2.28	-60:46:47.5	12.068	0.603	0.741	12852.0	12.450 ± 0.980	-
671	b	07:58: 2.28	-60:46:47.5	12.068	0.603	0.741	9296.3	13.660 ± 1.210	-
671	e	07:58: 2.28	-60:46:47.5	12.068	0.603	0.741	4886.2	19.240 ± 1.980	90%-99%
15503	c	07:58: 2.66	-60:48:48.1	8.950	0.080		17219.0	5.170 ± 0.550	-
15503	d	07:58: 2.66	-60:48:48.1	8.950	0.080		14876.0	3.630 ± 0.490	-
15503	f	07:58: 2.66	-60:48:48.1	8.950	0.080		13407.0	3.360 ± 0.500	-
15503	a	07:58: 2.66	-60:48:48.1	8.950	0.080		14800.0	6.820 ± 0.680	-
15503	b	07:58: 2.66	-60:48:48.1	8.950	0.080		10749.0	4.370 ± 0.640	-
675	d	07:58: 4.46	-60:38:25.9	18.829	1.606	2.386	9716.3	3.090 ± 0.560	-

the detections having less than 190 counts and only 23 detections more than 300 counts.

In order to have a statistical evaluation of the X-ray variability, we applied the unbinned Kolmogorov-Smirnov (K-S) test to the X-ray photon time series of our detected sources for each observation. Column 10 of Table 2 reports the results in terms of the confidence level at which we can reject the hypothesis that the source in the given observation is constant. Since the exposure times of the observations are in the 6 - 22.3 ksec range, we will refer to this analysis as short-time-scale variability. For each observation, we also ran the K-S test on the counts detected in the background regions to monitor possible background variability. In the few cases in which the background counts

are variable with a confidence level (CL) > 99%, the background counts are much lower than those of the source, making us confident of the results of the test variability.

Table 3 summarises the K-S test results for the total sample of X-ray sources (column 2), for the members (column 3), and for non-members (column 4). Among cluster members, only a small fraction (12%) of stars are variable with a CL ≥99%, while 73% are not variable (CL <90%); variability on a short-time-scale is not very common in NGC 2516, at least given the statistics of our observations. Table 4 and Figure 1 summarise the K-S test results for member stars of different spectral types; dF stars are the sources with the highest rate of variability (although the sample is very small), dG are those that are less variable.

**Table 2.** Continued

JTH	Obs.	Ra <sub>ott</sub> J2000	Dec <sub>ott</sub> J2000	V	B-V	V-I	Exposure [sec]	Rate ± err cnt/ks	K-S
676	<i>d</i>	07:58: 4.68	-60:52:42.7	18.790	1.602	2.442	11801.0	5.850 ± 0.700	≥99%
676	<i>f</i>	07:58: 4.68	-60:52:42.7	18.790	1.602	2.442	10287.0	3.890 ± 0.610	-
679	<i>c</i>	07:58: 5.40	-60:46:14.2	14.035	1.006	1.124	19333.0	5.070 ± 0.510	90%-99%
679	<i>d</i>	07:58: 5.40	-60:46:14.2	14.035	1.006	1.124	15578.0	3.020 ± 0.440	-
679	<i>a</i>	07:58: 5.40	-60:46:14.2	14.035	1.006	1.124	12181.0	15.020 ± 1.110	≥99%
679	<i>b</i>	07:58: 5.40	-60:46:14.2	14.035	1.006	1.124	8864.7	6.660 ± 0.870	-
681	<i>d</i>	07:58: 5.59	-60:45: 3.4	12.696	0.637	0.743	15286.0	3.140 ± 0.450	-
681	<i>f</i>	07:58: 5.59	-60:45: 3.4	12.696	0.637	0.743	14883.0	3.230 ± 0.470	-
686	<i>c</i>	07:58: 7.03	-60:48:26.1	17.567		2.412	17755.0	5.070 ± 0.530	-
686	<i>d</i>	07:58: 7.03	-60:48:26.1	17.567		2.412	15405.0	4.280 ± 0.530	90%-99%
686	<i>f</i>	07:58: 7.03	-60:48:26.1	17.567		2.412	14058.0	4.480 ± 0.560	-
686	<i>b</i>	07:58: 7.03	-60:48:26.1	17.567		2.412	10458.0	7.650 ± 0.860	≥99%
686	<i>d</i>	07:58: 7.46	-60:48:25.3	17.567		2.412	15405.0	4.280 ± 0.530	90%-99%
686	<i>f</i>	07:58: 7.46	-60:48:25.3	17.567		2.412	14058.0	4.480 ± 0.560	-
686	<i>b</i>	07:58: 7.46	-60:48:25.3	17.567		2.412	10458.0	7.650 ± 0.860	≥99%
691	<i>c</i>	07:58: 8.81	-60:44:38.0	12.220	0.560	0.676	19737.0	7.800 ± 0.630	-
691	<i>d</i>	07:58: 8.81	-60:44:38.0	12.220	0.560	0.676	15361.0	8.850 ± 0.760	-
691	<i>f</i>	07:58: 8.81	-60:44:38.0	12.220	0.560	0.676	15093.0	4.040 ± 0.520	-
691	<i>a</i>	07:58: 8.81	-60:44:38.0	12.220	0.560	0.676	10595.0	8.020 ± 0.870	90%-99%
691	<i>b</i>	07:58: 8.81	-60:44:38.0	12.220	0.560	0.676	7705.2	11.160 ± 1.200	-
691	<i>e</i>	07:58: 8.81	-60:44:38.0	12.220	0.560	0.676	4861.0	10.290 ± 1.450	-
15504	<i>c</i>	07:58: 10.30	-60:51:58.5	9.510	0.210		13858.0	9.240 ± 0.820	-
15504	<i>d</i>	07:58: 10.30	-60:51:58.5	9.510	0.210		13054.0	7.810 ± 0.770	-
15504	<i>f</i>	07:58: 10.30	-60:51:58.5	9.510	0.210		11190.0	10.460 ± 0.970	-
15504	<i>a</i>	07:58: 10.30	-60:51:58.5	9.510	0.210		17296.0	9.890 ± 0.760	-
15504	<i>b</i>	07:58: 10.30	-60:51:58.5	9.510	0.210		12457.0	8.430 ± 0.820	-
15504	<i>e</i>	07:58: 10.30	-60:51:58.5	9.510	0.210		4096.8	7.320 ± 1.340	-
696	<i>c</i>	07:58: 10.85	-60:49:33.2	12.036	0.532	0.682	16684.0	2.040 ± 0.350	-
698	<i>d</i>	07:58: 11.83	-60:50: 0.1	13.903	0.861	0.953	14592.0	4.590 ± 0.560	-
702	<i>c</i>	07:58: 12.26	-60:38:40.3	11.986	0.458	0.598	14505.0	4.690 ± 0.570	-
702	<i>d</i>	07:58: 12.26	-60:38:40.3	11.986	0.458	0.598	10128.0	8.590 ± 0.920	≥99%
702	<i>f</i>	07:58: 12.26	-60:38:40.3	11.986	0.458	0.598	11399.0	4.740 ± 0.640	-
712	<i>d</i>	07:58: 13.78	-60:45:20.8	10.117	0.149	0.168	15942.0	2.070 ± 0.360	-
15505	<i>c</i>	07:58: 14.71	-60:43:34.0	9.690	0.230		19354.0	1.525 ± 0.281	-
15505	<i>f</i>	07:58: 14.71	-60:43:34.0	9.690	0.230		15489.0	2.455 ± 0.398	-
15505	<i>b</i>	07:58: 14.71	-60:43:34.0	9.690	0.230		6883.5	2.105 ± 0.553	-
711	<i>c</i>	07:58: 14.71	-60:43:34.0	9.710	0.214	0.285	19354.0	1.525 ± 0.281	-
711	<i>f</i>	07:58: 14.71	-60:43:34.0	9.710	0.214	0.285	15489.0	2.455 ± 0.398	-
711	<i>b</i>	07:58: 14.71	-60:43:34.0	9.710	0.214	0.285	6883.5	2.105 ± 0.553	-
714	<i>a</i>	07:58: 15.48	-60:50:28.8	20.802		3.163	16263.0	2.150 ± 0.360	≥99%
720	<i>a</i>	07:58: 16.56	-60:52:12.2	18.862		2.514	17349.0	3.630 ± 0.460	≥99%
721	<i>c</i>	07:58: 16.58	-60:46:52.4	15.215	1.129	1.279	19249.0	2.700 ± 0.370	-
721	<i>f</i>	07:58: 16.58	-60:46:52.4	15.215	1.129	1.279	15599.0	2.630 ± 0.410	-
721	<i>a</i>	07:58: 16.58	-60:46:52.4	15.215	1.129	1.279	12921.0	2.400 ± 0.430	90%-99%
725	<i>c</i>	07:58: 18.26	-60:45:14.1	11.465	0.533	0.665	19970.0	11.020 ± 0.740	-
725	<i>d</i>	07:58: 18.26	-60:45:14.1	11.465	0.533	0.665	15462.0	9.960 ± 0.800	90%-99%
725	<i>f</i>	07:58: 18.26	-60:45:14.1	11.465	0.533	0.665	16273.0	13.700 ± 0.920	-
725	<i>a</i>	07:58: 18.26	-60:45:14.1	11.465	0.533	0.665	11182.0	11.720 ± 1.020	-
725	<i>b</i>	07:58: 18.26	-60:45:14.1	11.465	0.533	0.665	8123.9	9.110 ± 1.060	-
725	<i>e</i>	07:58: 18.26	-60:45:14.1	11.465	0.533	0.665	5087.8	9.240 ± 1.350	-
731	<i>c</i>	07:58: 19.15	-60:52: 0.2	15.246	1.136	1.234	13919.0	2.800 ± 0.450	90%-99%
731	<i>f</i>	07:58: 19.15	-60:52: 0.2	15.246	1.136	1.234	11553.0	2.250 ± 0.440	-
731	<i>e</i>	07:58: 19.15	-60:52: 0.2	15.246	1.136	1.234	3848.2	8.060 ± 1.450	-
735	<i>c</i>	07:58: 19.90	-60:42: 0.2	12.336	0.583	0.709	18046.0	11.300 ± 0.790	-
735	<i>d</i>	07:58: 19.90	-60:42: 0.2	12.336	0.583	0.709	13716.0	8.310 ± 0.780	-
735	<i>f</i>	07:58: 19.90	-60:42: 0.2	12.336	0.583	0.709	14664.0	9.750 ± 0.820	-
735	<i>a</i>	07:58: 19.90	-60:42: 0.2	12.336	0.583	0.709	8163.5	6.000 ± 0.860	-

In contrast, Wolk et al. (2004) find that the dF and B in their sample have the lowest rate of variability. Frequency of the variability on a short-time-scale is approximately equal among late- and early-types stars. The fraction of sources with significant variability is very small for each spectral type suggesting that, on short time scales, the properties of variability do not depend strongly on the mass. However, the sensitivity to variability depends on count statistics, and the absence of variability in faint stars may be not intrinsic but instead due to low counting statistics. Also the comparisons of our results with those obtained for other sample stars are limited by different statistics.

### 3.1. Time X-ray distribution functions

We derived the time amplitude X-ray luminosity distribution function (Time XAD) for the dF7-dK2 ( $0.5 \leq B-V \leq 0.99$ ) and dK3-dM ( $B-V > 0.9$ ) stars as in Marino et al. (2003b). Time XAD yields the fraction of time that a star spends with a count rate higher, by a given factor, than its minimum value. This distribution is constructed by considering for each star the ratio between the count rate observed during a given observation and the minimum rate for that source. We computed the Time XAD on a given time scale considering only observations obtained at a time separation of the order of the time scale we want to study. For example, if we want to study a

**Table 2.** Continued

JTH	Obs.	Ra <sub>ott</sub> J2000	Dec <sub>ott</sub> J2000	V	B-V	V-I	Exposure [sec]	Rate ± err cnt/ks	K-S
735	<i>b</i>	07:58:19.90	-60:42: 0.2	12.336	0.583	0.709	5925.9	10.630 ± 1.340	-
735	<i>e</i>	07:58:19.90	-60:42: 0.2	12.336	0.583	0.709	4277.9	7.250 ± 1.300	-
737	<i>c</i>	07:58:20.16	-60:41:38.7	12.871	0.660	0.760	17697.0	2.030 ± 0.340	-
737	<i>d</i>	07:58:20.16	-60:41:38.7	12.871	0.660	0.760	13716.0	8.310 ± 0.780	-
737	<i>f</i>	07:58:20.16	-60:41:38.7	12.871	0.660	0.760	14664.0	9.750 ± 0.820	-
737	<i>e</i>	07:58:20.16	-60:41:38.7	12.871	0.660	0.760	4277.9	7.250 ± 1.300	-
740	<i>a</i>	07:58:21.22	-60:58:52.0	14.680	1.156	1.294	12726.0	2.670 ± 0.460	-
15506	<i>a</i>	07:58:22.51	-60:51:26.0	8.020	-0.020		15968.0	1.595 ± 0.316	90%-99%
15506	<i>b</i>	07:58:22.51	-60:51:26.0	8.020	-0.020		11457.0	1.615 ± 0.375	-
15506	<i>c</i>	07:58:22.51	-60:51:26.0	8.020	-0.020		14541.0	4.265 ± 0.542	90%-99%
15506	<i>d</i>	07:58:22.51	-60:51:26.0	8.020	-0.020		13558.0	7.415 ± 0.740	≥99%
15506	<i>e</i>	07:58:22.51	-60:51:26.0	8.020	-0.020		4315.4	7.185 ± 1.290	-
15506	<i>f</i>	07:58:22.51	-60:51:26.0	8.020	-0.020		12196.0	5.780 ± 0.688	-
15507	<i>c</i>	07:58:22.51	-60:51:26.0	7.180	0.010		14541.0	4.265 ± 0.542	90%-99%
15507	<i>d</i>	07:58:22.51	-60:51:26.0	7.180	0.010		13558.0	7.415 ± 0.740	≥99%
15507	<i>f</i>	07:58:22.51	-60:51:26.0	7.180	0.010		12196.0	5.780 ± 0.688	-
15507	<i>a</i>	07:58:22.51	-60:51:26.0	7.180	0.010		15968.0	1.595 ± 0.316	90%-99%
15507	<i>b</i>	07:58:22.51	-60:51:26.0	7.180	0.010		11457.0	1.615 ± 0.375	-
15507	<i>e</i>	07:58:22.51	-60:51:26.0	7.180	0.010		4315.4	7.185 ± 1.290	-
749	<i>a</i>	07:58:22.58	-60:48:27.2	19.980		3.110	14290.0	2.940 ± 0.450	-
746	<i>c</i>	07:58:23.14	-60:40:21.9	14.516	0.943	1.118	16270.0	16.530 ± 1.010	≥99%
746	<i>d</i>	07:58:23.14	-60:40:21.9	14.516	0.943	1.118	12487.0	18.820 ± 1.230	-
746	<i>f</i>	07:58:23.14	-60:40:21.9	14.516	0.943	1.118	13362.0	20.880 ± 1.250	90%-99%
746	<i>a</i>	07:58:23.14	-60:40:21.9	14.516	0.943	1.118	6868.8	13.250 ± 1.390	-
746	<i>b</i>	07:58:23.14	-60:40:21.9	14.516	0.943	1.118	4961.7	15.120 ± 1.750	≥99%
746	<i>e</i>	07:58:23.14	-60:40:21.9	14.516	0.943	1.118	3978.5	22.620 ± 2.380	-
747	<i>a</i>	07:58:23.45	-60:54:58.5	14.123	1.063	1.140	16211.0	12.555 ± 0.880	≥99%
747	<i>b</i>	07:58:23.45	-60:54:58.5	14.123	1.063	1.140	11801.0	13.090 ± 1.053	90%-99%
747	<i>c</i>	07:58:23.45	-60:54:58.5	14.123	1.063	1.140	10414.0	10.705 ± 1.014	-
747	<i>d</i>	07:58:23.45	-60:54:58.5	14.123	1.063	1.140	10048.0	11.495 ± 1.070	-
747	<i>e</i>	07:58:23.45	-60:54:58.5	14.123	1.063	1.140	3207.9	12.155 ± 1.947	-
747	<i>f</i>	07:58:23.45	-60:54:58.5	14.123	1.063	1.140	8768.8	12.775 ± 1.207	-
748	<i>c</i>	07:58:23.45	-60:54:58.5	14.120	1.065	1.141	10414.0	10.705 ± 1.014	-
748	<i>d</i>	07:58:23.45	-60:54:58.5	14.120	1.065	1.141	10048.0	11.495 ± 1.070	-
748	<i>f</i>	07:58:23.45	-60:54:58.5	14.120	1.065	1.141	8768.8	12.775 ± 1.207	-
748	<i>a</i>	07:58:23.45	-60:54:58.5	14.120	1.065	1.141	16211.0	12.555 ± 0.880	≥99%
748	<i>b</i>	07:58:23.45	-60:54:58.5	14.120	1.065	1.141	11801.0	13.090 ± 1.053	90%-99%
748	<i>e</i>	07:58:23.45	-60:54:58.5	14.120	1.065	1.141	3207.9	12.155 ± 1.947	-
751	<i>c</i>	07:58:23.81	-60:37:20.1	12.354	0.571	0.672	12635.0	7.440 ± 0.770	-
751	<i>d</i>	07:58:23.81	-60:37:20.1	12.354	0.571	0.672	9292.5	12.380 ± 1.150	-
751	<i>f</i>	07:58:23.81	-60:37:20.1	12.354	0.571	0.672	10288.0	9.820 ± 0.980	-
767	<i>c</i>	07:58:29.95	-60:49: 0.0	16.176	1.433	1.825	16927.0	6.850 ± 0.640	≥99%
767	<i>d</i>	07:58:29.95	-60:49: 0.0	16.176	1.433	1.825	15680.0	7.910 ± 0.710	-
767	<i>f</i>	07:58:29.95	-60:49: 0.0	16.176	1.433	1.825	14601.0	6.990 ± 0.690	-
767	<i>a</i>	07:58:29.95	-60:49: 0.0	16.176	1.433	1.825	14496.0	19.380 ± 1.160	≥99%
767	<i>b</i>	07:58:29.95	-60:49: 0.0	16.176	1.433	1.825	10465.0	13.860 ± 1.150	≥99%
767	<i>e</i>	07:58:29.95	-60:49: 0.0	16.176	1.433	1.825	4969.5	9.060 ± 1.350	-
766	<i>c</i>	07:58:30.10	-60:41:52.1	9.734	0.113	0.131	15908.0	7.170 ± 0.670	-
766	<i>d</i>	07:58:30.10	-60:41:52.1	9.734	0.113	0.131	13821.0	14.690 ± 1.030	-
766	<i>f</i>	07:58:30.10	-60:41:52.1	9.734	0.113	0.131	14701.0	9.120 ± 0.790	-
766	<i>a</i>	07:58:30.10	-60:41:52.1	9.734	0.113	0.131	7866.9	10.680 ± 1.170	90%-99%
766	<i>b</i>	07:58:30.10	-60:41:52.1	9.734	0.113	0.131	5733.6	10.810 ± 1.370	-
766	<i>e</i>	07:58:30.10	-60:41:52.1	9.734	0.113	0.131	4411.1	12.920 ± 1.710	-
774	<i>c</i>	07:58:31.08	-60:37:47.7	10.583	0.307	0.386	12896.0	5.510 ± 0.650	-
774	<i>d</i>	07:58:31.08	-60:37:47.7	10.583	0.307	0.386	9749.5	3.490 ± 0.600	-
774	<i>f</i>	07:58:31.08	-60:37:47.7	10.583	0.307	0.386	10772.0	4.180 ± 0.620	≥99%
776	<i>c</i>	07:58:31.66	-60:53:12.0	17.870	1.521	2.306	12055.0	2.985 ± 0.498	-

1-day time scale, we can consider Obs. *a*, *b*, *d*, and *e* of Table 1. In Figure 2 the Time XAD on short (< 1 day) time scale with that on a medium (17 months) time scale. The same plot for dF7-dM stars is shown in Figure 3. To explore the presence of variations on medium time scale amplitudes, we excluded the stars variable (CL ≥ 99%) on short time scales that could produce spurious variability. Both the dF7-dK2 and dK3-dM distributions on short and medium time scales appear very alike, indicating that medium-term variations, if they exist at all, must have a much larger amplitude than those on short time scales. The null hypothesis that the XADs on short and medium time scales of dF7-dK2 stars are drawn from the same parent distribution cannot be rejected.

### 3.2. Long-term variability

The Sun's 11-year activity cycle, as observed in optical, radio, ultraviolet, and X-ray bands, is a well-established phenomenon. In the soft X-ray bandpass, the flux varies by about one order of magnitude during the solar cycle (Kreplin et al. 1977; Peres et al. 2000). The amplitude variations of the Sun are strongly dependent on time scale, with the highest probability of observing high-amplitude variations, between 4 and 7.5 years (Micela & Marino 2003). On these time scales, typically the observed variations are on average of the order of 1 dex, but the spread is very wide with an 80% probability of detecting variations in the 0.1 – 1.8 dex range. Solar-like cycles

**Table 2.** Continued

JTH	Obs.	Ra <sub>ott</sub> J2000	Dec <sub>ott</sub> J2000	V	B-V	V-I	Exposure [sec]	Rate ± err cnt/ks	K-S
776	<i>d</i>	07:58:31.66	-60:53:12.0	17.870	1.521	2.306	11911.0	3.860 ± 0.569	-
776	<i>f</i>	07:58:31.66	-60:53:12.0	17.870	1.521	2.306	10101.0	3.020 ± 0.547	-
776	<i>a</i>	07:58:31.66	-60:53:12.0	17.870	1.521	2.306	16396.0	4.330 ± 0.514	-
776	<i>e</i>	07:58:31.66	-60:53:12.0	17.870	1.521	2.306	3802.3	4.075 ± 1.035	-
780	<i>c</i>	07:58:31.66	-60:53:12.0	14.762	0.996	1.139	12055.0	2.985 ± 0.498	-
780	<i>d</i>	07:58:31.66	-60:53:12.0	14.762	0.996	1.139	11911.0	3.860 ± 0.569	-
780	<i>f</i>	07:58:31.66	-60:53:12.0	14.762	0.996	1.139	10101.0	3.020 ± 0.547	-
780	<i>a</i>	07:58:31.66	-60:53:12.0	14.762	0.996	1.139	16396.0	4.330 ± 0.514	-
780	<i>e</i>	07:58:31.66	-60:53:12.0	14.762	0.996	1.139	3802.3	4.075 ± 1.035	-
784	<i>c</i>	07:58:32.09	-60:53:53.8	10.508	0.226	0.250	11321.0	4.150 ± 0.610	-
784	<i>a</i>	07:58:32.09	-60:53:53.8	10.508	0.226	0.250	16212.0	4.130 ± 0.500	90%-99%
784	<i>b</i>	07:58:32.09	-60:53:53.8	10.508	0.226	0.250	11781.0	5.690 ± 0.690	≥99%
787	<i>c</i>	07:58:32.26	-60:59:52.4	16.758	1.454	1.757	6385.4	4.850 ± 0.870	-
785	<i>d</i>	07:58:32.33	-60:46: 1.0	14.611	0.981	1.141	16627.0	15.880 ± 0.980	-
785	<i>f</i>	07:58:32.33	-60:46: 1.0	14.611	0.981	1.141	16625.0	10.770 ± 0.800	-
785	<i>a</i>	07:58:32.33	-60:46: 1.0	14.611	0.981	1.141	11318.0	9.630 ± 0.920	-
785	<i>b</i>	07:58:32.33	-60:46: 1.0	14.611	0.981	1.141	8270.5	10.040 ± 1.100	-
785	<i>e</i>	07:58:32.33	-60:46: 1.0	14.611	0.981	1.141	5299.5	25.100 ± 2.180	-
788	<i>f</i>	07:58:32.90	-60:48:52.5	17.528	1.565	1.974	14671.0	2.930 ± 0.450	-
789	<i>c</i>	07:58:33.07	-60:51:29.8	18.567		2.630	14140.0	1.840 ± 0.360	-
789	<i>d</i>	07:58:33.07	-60:51:29.8	18.567		2.630	13515.0	2.000 ± 0.380	90%-99%
789	<i>a</i>	07:58:33.07	-60:51:29.8	18.567		2.630	15511.0	2.390 ± 0.390	90%-99%
789	<i>e</i>	07:58:33.07	-60:51:29.8	18.567		2.630	4279.1	8.880 ± 1.440	≥99%
792	<i>c</i>	07:58:33.43	-60:44:27.9	12.841	0.691	0.836	18563.0	15.680 ± 0.920	-
792	<i>d</i>	07:58:33.43	-60:44:27.9	12.841	0.691	0.836	15847.0	15.140 ± 0.980	-
792	<i>f</i>	07:58:33.43	-60:44:27.9	12.841	0.691	0.836	16447.0	13.680 ± 0.910	-
792	<i>a</i>	07:58:33.43	-60:44:27.9	12.841	0.691	0.836	9981.4	16.830 ± 1.300	90%-99%
792	<i>b</i>	07:58:33.43	-60:44:27.9	12.841	0.691	0.836	7446.8	11.950 ± 1.270	-
792	<i>e</i>	07:58:33.43	-60:44:27.9	12.841	0.691	0.836	5052.4	9.100 ± 1.340	-
796	<i>c</i>	07:58:34.15	-60:38:23.7	20.279		2.995	13415.0	2.160 ± 0.400	≥99%
796	<i>f</i>	07:58:34.15	-60:38:23.7	20.279		2.995	11268.0	2.660 ± 0.490	-
799	<i>a</i>	07:58:34.70	-61:03:19.6	13.084	0.681	0.801	8182.6	5.500 ± 0.820	90%-99%
799	<i>b</i>	07:58:34.70	-61:03:19.6	13.084	0.681	0.801	5976.0	8.030 ± 1.160	-
800	<i>b</i>	07:58:35.38	-60:46:53.9	13.405	0.736	0.838	8872.9	11.270 ± 1.130	-
800	<i>e</i>	07:58:35.38	-60:46:53.9	13.405	0.736	0.838	5245.4	8.960 ± 1.310	-
800	<i>d</i>	07:58:35.83	-60:46:51.2	13.405	0.736	0.838	16487.0	14.860 ± 0.950	-
800	<i>f</i>	07:58:35.83	-60:46:51.2	13.405	0.736	0.838	15021.0	8.390 ± 0.750	-
800	<i>a</i>	07:58:35.83	-60:46:51.2	13.405	0.736	0.838	12248.0	26.370 ± 1.470	-
800	<i>b</i>	07:58:35.83	-60:46:51.2	13.405	0.736	0.838	8872.9	11.270 ± 1.130	-
800	<i>e</i>	07:58:35.83	-60:46:51.2	13.405	0.736	0.838	5245.4	8.960 ± 1.310	-
803	<i>c</i>	07:58:36.55	-60:50:17.9	11.675	0.585	0.695	15296.0	12.290 ± 0.900	≥99%
803	<i>d</i>	07:58:36.55	-60:50:17.9	11.675	0.585	0.695	14474.0	12.090 ± 0.910	-
803	<i>f</i>	07:58:36.55	-60:50:17.9	11.675	0.585	0.695	12897.0	4.960 ± 0.620	-
803	<i>a</i>	07:58:36.55	-60:50:17.9	11.675	0.585	0.695	14915.0	6.970 ± 0.680	-
803	<i>b</i>	07:58:36.55	-60:50:17.9	11.675	0.585	0.695	10862.0	5.430 ± 0.710	-
803	<i>e</i>	07:58:36.55	-60:50:17.9	11.675	0.585	0.695	4605.1	6.730 ± 1.210	-
804	<i>f</i>	07:58:36.89	-60:48: 6.8	18.328	1.480	2.267	15229.0	3.550 ± 0.480	90%-99%
806	<i>f</i>	07:58:37.10	-60:46:23.6	15.217	1.121	1.242	16293.0	3.680 ± 0.480	-
806	<i>b</i>	07:58:37.10	-60:46:23.6	15.217	1.121	1.242	8482.0	7.430 ± 0.940	-
812	<i>c</i>	07:58:38.86	-60:48:23.6	16.885	1.441	1.837	16864.0	2.490 ± 0.380	90%-99%
816	<i>c</i>	07:58:40.32	-60:41:46.0	12.212	0.561	0.673	16350.0	2.810 ± 0.410	-
816	<i>d</i>	07:58:40.32	-60:41:46.0	12.212	0.561	0.673	13471.0	6.760 ± 0.710	90%-99%
816	<i>f</i>	07:58:40.32	-60:41:46.0	12.212	0.561	0.673	14456.0	4.980 ± 0.590	-
816	<i>a</i>	07:58:40.32	-60:41:46.0	12.212	0.561	0.673	7576.1	9.640 ± 1.130	≥99%
816	<i>b</i>	07:58:40.32	-60:41:46.0	12.212	0.561	0.673	5492.5	11.830 ± 1.470	-
820	<i>c</i>	07:58:41.78	-60:50:52.0	17.733	1.564	2.123	14301.0	3.220 ± 0.470	-
820	<i>d</i>	07:58:41.78	-60:50:52.0	17.7	1.564	2.123	13841.0	3.030 ± 0.470	-

have been observed in late-type stars from chromospheric flux variations (Wilson 1978; Baliunas et al. 1995). Only in more recent years, X-ray long-term variability possibly due to cyclical variations has been observed in stars (Hempelmann et al. 2003; Favata et al. 2004). By combining X-ray data obtained with ROSAT and, at present, XMM-Newton, we explored the long-term variability of the late-type stars of NGC 2516.

Thirty-eight late-type stars (dF7-dM) of the cluster observed with XMM-Newton were observed with ROSAT/PSPC in 1993 (Jeffries et al. 1997) and twenty-three with ROSAT/HRI in 1997 (Micela et al. 2000), allowing us to explore variability on 7-8 and 4-5 year time scales, respectively. In order to compare our results with

ROSAT observations, we derived EPIC/pn X-ray luminosities in the(0.15-2.0) keV bandpass, assuming a constant conversion factor to convert count rates to flux, as more extensively described in Sect. 3.3. For each star, several points were available from EPIC/pn and only one from PSPC ( $L_{PSPC}$ ) and HRI ( $L_{HRI}$ ). We reduced the influence of short and medium variability in the EPIC/pn data, averaging the latter to a single mean value ( $L_{pn}$ ). The amplitude of variability is defined as  $\log(L_x/L_{xmin})$ , where  $L_x$  is the higher and  $L_{xmin}$ , the lower value between  $L_{pn}$  and  $L_{PSPC}$  and between  $L_{pn}$  and  $L_{HRI}$ , respectively. Figure 4 shows the XADs of the stars observed both with PSPC and EPIC/pn observations, and with HRI and EPIC/pn. For comparison in the same figure, we

**Table 2.** Continued

JTH	Obs.	Ra <sub>ott</sub> J2000	Dec <sub>ott</sub> J2000	V	B-V	V-I	Exposure [sec]	Rate ± err cnt/ks	K-S
820	<i>f</i>	07:58:41.78	-60:50:52.0	17.733	1.564	2.123	12899.0	4.650 ± 0.600	-
820	<i>b</i>	07:58:41.78	-60:50:52.0	17.733	1.564	2.123	10667.0	3.660 ± 0.590	-
823	<i>f</i>	07:58:42.84	-60:40:20.4	13.641	0.781	0.851	13214.0	1.970 ± 0.390	-
826	<i>c</i>	07:58:43.39	-60:55:26.8	13.840	0.818	0.963	9528.0	16.900 ± 1.330	-
826	<i>d</i>	07:58:43.39	-60:55:26.8	13.840	0.818	0.963	9315.6	28.120 ± 1.740	90%-99%
826	<i>f</i>	07:58:43.39	-60:55:26.8	13.840	0.818	0.963	8385.0	66.070 ± 2.810	≥99%
826	<i>a</i>	07:58:43.39	-60:55:26.8	13.840	0.818	0.963	14433.0	40.880 ± 1.680	90%-99%
826	<i>b</i>	07:58:43.39	-60:55:26.8	13.840	0.818	0.963	10518.0	24.530 ± 1.530	-
826	<i>e</i>	07:58:43.39	-60:55:26.8	13.840	0.818	0.963	2969.9	28.960 ± 3.120	-
828	<i>c</i>	07:58:43.70	-60:32:57.7	12.607	0.762	0.864	7842.7	13.010 ± 1.290	-
828	<i>d</i>	07:58:43.70	-60:32:57.7	12.607	0.762	0.864	5933.9	9.610 ± 1.270	-
828	<i>e</i>	07:58:43.70	-60:32:57.7	12.607	0.762	0.864	1890.0	15.870 ± 2.900	-
830	<i>c</i>	07:58:43.87	-60:45:36.0	17.859	1.597	2.263	17424.0	2.410 ± 0.370	≥99%
830	<i>d</i>	07:58:43.87	-60:45:36.0	17.859	1.597	2.263	15736.0	1.590 ± 0.320	-
840	<i>c</i>	07:58:48.22	-60:54:15.7	14.335	0.903	1.048	10277.0	24.330 ± 1.540	-
840	<i>d</i>	07:58:48.22	-60:54:15.7	14.335	0.903	1.048	10331.0	17.910 ± 1.320	-
840	<i>f</i>	07:58:48.22	-60:54:15.7	14.335	0.903	1.048	9248.1	15.460 ± 1.290	-
840	<i>a</i>	07:58:48.22	-60:54:15.7	14.335	0.903	1.048	14560.0	24.930 ± 1.310	≥99%
840	<i>b</i>	07:58:48.22	-60:54:15.7	14.335	0.903	1.048	10595.0	17.460 ± 1.280	90%-99%
840	<i>e</i>	07:58:48.22	-60:54:15.7	14.335	0.903	1.048	3276.2	19.840 ± 2.460	-
845	<i>d</i>	07:58:48.84	-60:47:47.6	18.489	1.561	2.476	15257.0	2.880 ± 0.430	-
845	<i>a</i>	07:58:48.84	-60:47:47.6	18.489	1.561	2.476	12104.0	4.460 ± 0.610	90%-99%
843	<i>d</i>	07:58:48.89	-60:55:24.9	11.954	0.515	0.587	9204.5	3.040 ± 0.570	-
15510	<i>c</i>	07:58:50.35	-60:38:38.9	9.510	0.080		12580.0	39.750 ± 1.780	90%-99%
15510	<i>d</i>	07:58:50.35	-60:38:38.9	9.510	0.080		10014.0	37.750 ± 1.940	-
15510	<i>f</i>	07:58:50.35	-60:38:38.9	9.510	0.080		11126.0	85.120 ± 2.770	≥99%
15510	<i>a</i>	07:58:50.35	-60:38:38.9	9.510	0.080		5465.2	37.510 ± 2.620	-
15510	<i>b</i>	07:58:50.35	-60:38:38.9	9.510	0.080		3971.8	36.760 ± 3.040	-
15510	<i>e</i>	07:58:50.35	-60:38:38.9	9.510	0.080		3200.7	39.370 ± 3.510	-
15509	<i>c</i>	07:58:50.62	-60:49:29.6	5.800	-0.090		14776.0	43.720 ± 1.720	-
15509	<i>d</i>	07:58:50.62	-60:49:29.6	5.800	-0.090		14265.0	31.900 ± 1.500	≥99%
15509	<i>f</i>	07:58:50.62	-60:49:29.6	5.800	-0.090		13623.0	38.900 ± 1.690	-
15509	<i>a</i>	07:58:50.62	-60:49:29.6	5.800	-0.090		13202.0	49.310 ± 1.930	≥99%
15509	<i>b</i>	07:58:50.62	-60:49:29.6	5.800	-0.090		9570.4	26.540 ± 1.670	-
15509	<i>e</i>	07:58:50.62	-60:49:29.6	5.800	-0.090		4530.5	39.730 ± 2.960	-
855	<i>c</i>	07:58:51.91	-60:35:20.8	14.781	0.988	1.127	9512.1	13.670 ± 1.200	-
855	<i>d</i>	07:58:51.91	-60:35:20.8	14.781	0.988	1.127	7383.2	13.140 ± 1.330	-
855	<i>f</i>	07:58:51.91	-60:35:20.8	14.781	0.988	1.127	8193.0	14.520 ± 1.330	-
855	<i>e</i>	07:58:51.91	-60:35:20.8	14.781	0.988	1.127	2321.4	14.650 ± 2.510	-
856	<i>c</i>	07:58:52.51	-60:53:38.2	12.142	0.659	0.758	10672.0	8.250 ± 0.880	-
856	<i>d</i>	07:58:52.51	-60:53:38.2	12.142	0.659	0.758	10672.0	7.780 ± 0.850	-
856	<i>f</i>	07:58:52.51	-60:53:38.2	12.142	0.659	0.758	9749.9	8.000 ± 0.910	-
856	<i>a</i>	07:58:52.51	-60:53:38.2	12.142	0.659	0.758	14142.0	7.280 ± 0.720	90%-99%
856	<i>b</i>	07:58:52.51	-60:53:38.2	12.142	0.659	0.758	10281.0	6.610 ± 0.800	-
856	<i>e</i>	07:58:52.51	-60:53:38.2	12.142	0.659	0.758	3389.3	8.260 ± 1.560	-
860	<i>c</i>	07:58:52.94	-60:36:11.8	9.781	0.185	0.239	10115.0	11.270 ± 1.060	-
860	<i>d</i>	07:58:52.94	-60:36:11.8	9.781	0.185	0.239	8000.8	12.120 ± 1.230	-
860	<i>f</i>	07:58:52.94	-60:36:11.8	9.781	0.185	0.239	8825.6	14.390 ± 1.280	-
860	<i>e</i>	07:58:52.94	-60:36:11.8	9.781	0.185	0.239	2550.5	11.760 ± 2.150	-
864	<i>a</i>	07:58:53.38	-60:56:33.8	18.389	1.562	2.624	12862.0	2.640 ± 0.450	90%-99%
864	<i>b</i>	07:58:53.38	-60:56:33.8	18.389	1.562	2.624	9289.2	4.950 ± 0.730	-
862	<i>c</i>	07:58:53.93	-60:54:23.7	16.856	1.527	2.088	9953.0	3.620 ± 0.600	-
862	<i>d</i>	07:58:53.93	-60:54:23.7	16.856	1.527	2.088	9906.4	7.970 ± 0.900	90%-99%
862	<i>f</i>	07:58:53.93	-60:54:23.7	16.856	1.527	2.088	8954.2	5.700 ± 0.800	90%-99%
862	<i>a</i>	07:58:53.93	-60:54:23.7	16.856	1.527	2.088	13868.0	5.190 ± 0.610	90%-99%
862	<i>b</i>	07:58:53.93	-60:54:23.7	16.856	1.527	2.088	10117.0	5.040 ± 0.710	-
868	<i>d</i>	07:58:56.50	-60:47:22.3	17.183	1.492	1.930	14544.0	1.790 ± 0.350	90%-99%

also show the XADs limited to EPIC/pn dF7-dM stars on time scales of 1 day and on 17 months. The XADs on time scales of 4-5 years and on 7-8 years are marginally ( $CL \geq 96\%$ ) different, suggesting that long-term variations could be present. However, long-term variations, if they exist, must have a smaller amplitude than the short and medium term variations, or comparable to them. Our finding that there is no evidence of significant long-term variability agrees with those for other samples of young stars (e.g. Gagné et al. 1995; Marino et al. 2003b; Pillitteri et al. 2004; Stern et al. 1995; Marino et al. 2005), supporting a scenario in which stars much younger than the Sun (i.e. at ages  $\lesssim 1$  Gyr) do not have long-term cycles or their cycle amplitudes are much smaller than the solar one. On

the other hand, there is growing evidence that cycles are present in older stars having age comparable to the solar one (Hempelmann et al. 2003; Favata et al. 2004).

### 3.3. Comparison with the Pleiades

The X-ray emission level decreases with increasing age as an effect of rotational braking (e.g. Micela et al. 1985, 1990, 1996; Barbera et al. 1993; Stauffer et al. 1994; Maggio et al. 1987). A decrease by three dex in the median value of  $L_x$  with a spread of about 1 dex was observed in coeval stars. How much of this spread is due to variability and both if and how variability properties change with age is not clear. Comparing clusters of a very similar age is

**Table 2.** Continued

JTH	Obs.	Ra <sub>ott</sub> J2000	Dec <sub>ott</sub> J2000	V	B-V	V-I	Exposure [sec]	Rate ± err cnt/ks	K-S
868	<i>b</i>	07:58:56.50	-60:47:22.3	17.183	1.492	1.930	8064.1	4.840 ± 0.770	-
870	<i>c</i>	07:58:57.17	-60:36:13.6	14.867	1.034	1.171	9930.8	10.880 ± 1.050	-
870	<i>d</i>	07:58:57.17	-60:36:13.6	14.867	1.034	1.171	7865.9	6.610 ± 0.920	-
870	<i>f</i>	07:58:57.17	-60:36:13.6	14.867	1.034	1.171	8677.2	10.030 ± 1.070	-
871	<i>a</i>	07:58:57.74	-60:43: 3.6	14.760	0.990	1.140	7847.0	26.700 ± 1.845	≥99%
871	<i>c</i>	07:58:57.74	-60:43: 3.6	14.760	0.990	1.140	15135.0	9.975 ± 0.812	90%-99%
871	<i>b</i>	07:58:57.74	-60:43: 3.6	14.760	0.990	1.140	5703.3	7.275 ± 1.129	-
871	<i>d</i>	07:58:57.74	-60:43: 3.6	14.760	0.990	1.140	13353.0	8.165 ± 0.782	≥99%
871	<i>e</i>	07:58:57.74	-60:43: 3.6	14.760	0.990	1.140	4225.0	6.980 ± 1.285	-
871	<i>f</i>	07:58:57.74	-60:43: 3.6	14.760	0.990	1.140	14204.0	7.005 ± 0.702	-
873	<i>c</i>	07:58:57.74	-60:43: 3.6	19.089	2.804	15135.0	9.975 ± 0.812	90%-99%	
873	<i>d</i>	07:58:57.74	-60:43: 3.6	19.089	2.804	13353.0	8.165 ± 0.782	≥99%	
873	<i>f</i>	07:58:57.74	-60:43: 3.6	19.089	2.804	14204.0	7.005 ± 0.702	-	
873	<i>a</i>	07:58:57.74	-60:43: 3.6	19.089	2.804	7847.0	26.700 ± 1.845	≥99%	
873	<i>b</i>	07:58:57.74	-60:43: 3.6	19.089	2.804	5703.3	7.275 ± 1.129	-	
873	<i>e</i>	07:58:57.74	-60:43: 3.6	19.089	2.804	4225.0	6.980 ± 1.285	-	
884	<i>f</i>	07:59:02.78	-60:47:46.9	10.781	0.281	0.328	13896.0	2.450 ± 0.420	≥99%
896	<i>c</i>	07:59:06.02	-60:46:17.4	19.981	3.002	14197.0	1.900 ± 0.370	-	
896	<i>d</i>	07:59:06.02	-60:46:17.4	19.981	3.002	13538.0	1.920 ± 0.380	-	
897	<i>d</i>	07:59: 7.10	-60:52: 1.1	15.874	1.255	1.467	11002.0	4.000 ± 0.600	-
907	<i>d</i>	07:59:10.25	-60:50:53.1	17.516	1.442	2.082	11589.0	2.420 ± 0.460	-
907	<i>f</i>	07:59:10.25	-60:50:53.1	17.516	1.442	2.082	11094.0	4.240 ± 0.620	-
928	<i>d</i>	07:59:15.98	-60:47:38.0	16.266	1.495	1.850	12312.0	2.270 ± 0.430	-
933	<i>c</i>	07:59:18.00	-60:45:21.2	17.771	1.625	2.378	12475.0	3.050 ± 0.490	-
933	<i>d</i>	07:59:18.00	-60:45:21.2	17.771	1.625	2.378	12017.0	4.080 ± 0.580	-
933	<i>f</i>	07:59:18.00	-60:45:21.2	17.771	1.625	2.378	12667.0	2.450 ± 0.440	-
933	<i>a</i>	07:59:18.00	-60:45:21.2	17.771	1.625	2.378	8088.9	3.090 ± 0.620	-
940	<i>c</i>	07:59:19.70	-60:34:43.4	11.936	0.525	0.653	7437.6	58.490 ± 2.800	≥99%
940	<i>d</i>	07:59:19.70	-60:34:43.4	11.936	0.525	0.653	6053.5	5.620 ± 0.960	-
940	<i>f</i>	07:59:19.70	-60:34:43.4	11.936	0.525	0.653	6843.2	6.140 ± 0.950	-
944	<i>d</i>	07:59:21.26	-60:50:53.4	19.283	2.881	2.881	10422.0	10.750 ± 1.020	≥99%
944	<i>a</i>	07:59:21.26	-60:50:53.4	19.283	2.881	10414.0	3.170 ± 0.550	-	
944	<i>b</i>	07:59:21.26	-60:50:53.4	19.283	2.881	7520.5	5.450 ± 0.850	≥99%	
945	<i>c</i>	07:59:21.31	-60:46: 3.2	12.341	0.569	0.695	12057.0	4.480 ± 0.610	-
945	<i>d</i>	07:59:21.31	-60:46: 3.2	12.341	0.569	0.695	11714.0	5.720 ± 0.700	-
945	<i>f</i>	07:59:21.31	-60:46: 3.2	12.341	0.569	0.695	11693.0	3.930 ± 0.580	-
945	<i>a</i>	07:59:21.31	-60:46: 3.2	12.341	0.569	0.695	8143.4	12.400 ± 1.230	≥99%
945	<i>b</i>	07:59:21.31	-60:46: 3.2	12.341	0.569	0.695	5923.3	5.400 ± 0.960	-
15512	<i>c</i>	07:59:21.46	-60:48:57.9	9.110	0.030		11042.0	19.560 ± 1.330	90%-99%
15512	<i>d</i>	07:59:21.46	-60:48:57.9	9.110	0.030		10704.0	14.850 ± 1.180	90%-99%
15512	<i>f</i>	07:59:21.46	-60:48:57.9	9.110	0.030		11358.0	17.960 ± 1.260	≥99%
15512	<i>a</i>	07:59:21.46	-60:48:57.9	9.110	0.030		9480.3	19.090 ± 1.420	-
15512	<i>b</i>	07:59:21.46	-60:48:57.9	9.110	0.030		6909.1	28.220 ± 2.020	-
15512	<i>e</i>	07:59:21.46	-60:48:57.9	9.110	0.030		3475.9	10.930 ± 1.770	-
947	<i>c</i>	07:59:21.67	-60:46:47.7	14.509	0.976	1.061	11781.0	3.060 ± 0.510	-
947	<i>d</i>	07:59:21.67	-60:46:47.7	14.509	0.976	1.061	11465.0	2.180 ± 0.440	-
950	<i>c</i>	07:59:22.39	-60:45:27.1	11.873	0.616		11841.0	8.190 ± 0.830	-
950	<i>d</i>	07:59:22.39	-60:45:27.1	11.873	0.616		11525.0	7.900 ± 0.830	-
950	<i>f</i>	07:59:22.39	-60:45:27.1	11.873	0.616		11521.0	2.690 ± 0.480	≥99%
950	<i>a</i>	07:59:22.39	-60:45:27.1	11.873	0.616		7810.1	5.510 ± 0.840	-
954	<i>c</i>	07:59:24.05	-60:34:34.1	17.699	1.610	2.308	7049.8	4.110 ± 0.760	-
963	<i>c</i>	07:59:27.19	-60:47:55.0	9.639	0.075	0.084	10273.0	3.990 ± 0.620	≥99%
963	<i>d</i>	07:59:27.19	-60:47:55.0	9.639	0.075	0.084	10724.0	6.060 ± 0.750	-
963	<i>f</i>	07:59:27.19	-60:47:55.0	9.639	0.075	0.084	10914.0	4.860 ± 0.670	-
963	<i>a</i>	07:59:27.19	-60:47:55.0	9.639	0.075	0.084	8471.4	5.430 ± 0.800	≥99%
963	<i>b</i>	07:59:27.19	-60:47:55.0	9.639	0.075	0.084	6166.3	9.730 ± 1.260	-
963	<i>e</i>	07:59:27.19	-60:47:55.0	9.639	0.075	0.084	3425.1	8.470 ± 1.570	90%-99%

very useful for testing the evolutionary scenario. However ROSAT observations have shown that clusters of the same age may have significantly different levels of X-ray emission. For instance, late type-stars in the Praesepe cluster are much weaker emitter in X-rays than the Hyades stars (Randich et al. 1995), despite the fact that they have the same age and chemical composition as the Hyades. Many attempts have been made to explain the observed difference, but this puzzle has not yet been totally solved. An observation of the Praesepe cluster obtained with XMM-Newton (Franciosini et al. 2003) supports the hypothesis that Praesepe may be formed by two merging clusters with different ages.

We compared NGC 2516 with the slightly younger Pleiades; in particular, we compared the Time XADs of dF7-dK2 and dK3-dM members of NGC 2516 with the analogous ones for the Pleiades (Marino et al. 2003b). We converted EPIC/pn count rates to flux in the 0.1-2.4 keV ROSAT energy band. In deriving X-ray flux we assumed a constant conversion factor of  $4.0 \times 10^{-12}$  erg cm $^{-2}$ /count for the pn camera, computed with PIMMS, for a 1-T Raymond-Smith spectrum with a temperature of logT=6.80 K, and a fixed  $N_H = 7.5 \times 10^{20}$  cm $^{-2}$  corresponding to the cluster extinction  $A_V = 0.37$  (Jeffries et al. 2001). Figure 5 shows the Time XADs of dF7-dK2 in NGC 2516 and Pleiades: the two distributions appear marginally different, with the Pleiades dF7-dK2 ampli-

**Table 2.** Continued

JTH	Obs.	Ra <sub>ott</sub> J2000	Dec <sub>ott</sub> J2000	V	B-V	V-I	Exposure [sec]	Rate ± err cnt/ks	K-S
967	c	07:59:28.97	-60:39:36.8	17.410	1.520	2.006	9534.9	2.940 ± 0.550	≥99%
977	c	07:59:32.04	-60:48:47.2	13.879	0.834	1.019	9887.9	27.510 ± 1.670	90%-99%
977	d	07:59:32.04	-60:48:47.2	13.879	0.834	1.019	9696.1	22.380 ± 1.520	90%-99%
977	f	07:59:32.04	-60:48:47.2	13.879	0.834	1.019	10348.0	20.680 ± 1.410	-
977	a	07:59:32.04	-60:48:47.2	13.879	0.834	1.019	8466.0	28.470 ± 1.830	-
977	b	07:59:32.04	-60:48:47.2	13.879	0.834	1.019	6154.6	27.620 ± 2.120	-
977	e	07:59:32.04	-60:48:47.2	13.879	0.834	1.019	3150.8	18.410 ± 2.420	90%-99%
979	a	07:59:32.04	-60:58:48.9	14.995	1.048	1.177	7890.8	5.830 ± 0.860	-
979	b	07:59:32.04	-60:58:48.9	14.995	1.048	1.177	5727.6	7.330 ± 1.130	-
999	c	07:59:40.03	-60:42:33.8	14.774	1.046	1.206	9379.7	6.180 ± 0.810	90%-99%
999	d	07:59:40.03	-60:42:33.8	14.774	1.046	1.206	8672.4	5.190 ± 0.770	-
999	f	07:59:40.03	-60:42:33.8	14.774	1.046	1.206	9363.2	8.440 ± 0.950	-
1012	f	07:59:47.52	-60:44:52.7	17.354	1.489	2.040	8957.6	5.360 ± 0.770	-
1012	f	07:59:48.43	-60:44:53.7	17.354	1.489	2.040	8957.6	5.360 ± 0.770	-
1035	c	07:59:55.78	-60:41:53.7	10.780	0.318	0.395	7594.7	8.430 ± 1.050	≥99%
1035	d	07:59:55.78	-60:41:53.7	10.780	0.318	0.395	7138.8	5.320 ± 0.860	-
1035	f	07:59:55.78	-60:41:53.7	10.780	0.318	0.395	7750.9	4.640 ± 0.770	-
1035	a	07:59:55.78	-60:41:53.7	10.780	0.318	0.395	5105.8	10.770 ± 1.450	≥99%
1040	c	07:59:56.90	-60:49:27.8	11.648	0.623	0.615	7234.6	4.700 ± 0.810	-
1040	a	07:59:56.90	-60:49:27.8	11.648	0.623	0.615	6421.4	4.050 ± 0.790	-
1040	b	07:59:56.90	-60:49:27.8	11.648	0.623	0.615	4677.5	5.990 ± 1.130	-
1054	a	08:00: 2.45	-60:53:51.1	19.568		2.953	6416.5	9.820 ± 1.240	≥99%
1097	c	08:00:20.57	-60:42:35.7	13.488	0.927	1.051	5936.9	9.770 ± 1.280	-

**Table 3.** Results of the K-S test for each X-ray detected source.

Confidence <sup>1</sup> level	Number of total sources	Number of cluster members	Number of non members
<90%	490 (74%)	345 (73%)	145 (79%)
90%-99%	96 (15%)	72 (15%)	24 (13%)
≥ 99%	71 (11%)	57 (12%)	14 (8%)

<sup>1</sup>Confidence level for the rejection of the constant source hypothesis.

**Table 4.** Results of the K-S test for the stars of NGC 2516 grouped by spectral type.

Confidence <sup>1</sup> level	Number of cluster members					
	B	dA	dF	dG	dK	dM
<90%	9 (64%)	62 (74%)	9 (69%)	109 (83%)	119 (70%)	37 (59%)
90%-99%	2 (14%)	13 (15%)	0	14 (11%)	32 (19%)	11 (17%)
≥ 99%	3 (22%)	9 (11%)	4(31%)	8 (6%)	18 (11%)	15 (24%)

<sup>1</sup>Confidence level for the rejection of the constant source hypothesis.

tude of variations larger than those of NGC 2516 dF7-dK2. However, using the two sample K-S test, the null hypothesis that the two distributions came from the same parent distribution, can be rejected only at a CL ≥ 73%. Analogously, Time XADs of dK3-dM in NGC 2516 and Pleiades (Figure 6) show very similar amplitudes of variations, and the difference is marginal since the two distributions differ at a CL ≥ 92%. These results suggest that the amplitude variations both for dF7-dK2 and dK3-dM in NGC 2516 are consistent with the analogous distributions in the coeval Pleiades.

#### 4. Spectral variability

Spectral properties of stellar coronae of the cluster have been investigated in Pillitteri et al. (2006) by fitting the X-ray spectra of EPIC/pn simultaneously. They found that

spectra of G, K, and M type stars are described well with one or two thermal components, similar to other clusters, such as Pleiades (Briggs & Pye 2003), Blanco 1 (Pillitteri et al. 2004), IC 2391 (Marino et al. 2005), etc.

We searched for spectral variations in the cluster members for which more than one pn spectra were obtainable. Due to low counts for most of the sources, this search was possible only for three stars (Table 5). Two of them are early-type stars for which stellar structure models predict the lack of, or a very thin, convective zone (required to generate magnetic activity), and hence the lack of one key ingredient for an  $\alpha$ -Ω dynamo. Even though no X-ray emission is expected from these stars, the early-type JTH 15509 and JTH 15510 are the brightest sources in the EPIC field of view. JTH 15510, an A0 star flagged as single by Jeffries et al. (1997) in three of the six observations, have sufficient counts (more than 350) to obtain three sep-

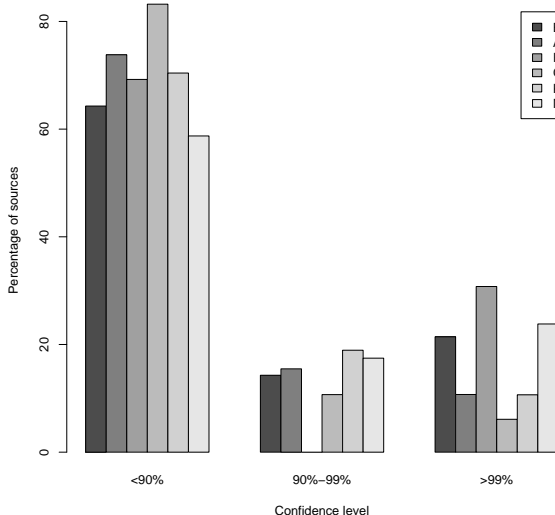


**Fig. 1.** Percentage of detected stars vs. variability confidence level and spectral type.

parate spectra (Figure 7). The two spectra concerning Obs. *c* and *d* are very similar, and simultaneous fits are possible, while the spectrum in the Obs. *f* is different, implying different physical conditions. As shown in Figure 8 the spectral variability in Obs. *f* corresponds to the presence of a flare in the light-curve, while the remaining two light-curves show no evidence of significant variability. The fits with the 2-T APEC model plus a photometric absorption provides for Obs. *c* and *d*, similar temperatures at  $\approx 0.39$  keV and  $1.00$  keV, with  $EM_{cold}/EM_{hot} \approx 1.2$  having fixed  $N_H = 6 \times 10^{20}$  cm $^{-2}$ , and assumed under-solar abundances at  $0.3 Z_\odot$ . To fit Obs. *f*, a third hotter temperature component must be added to the model that fits Obs. *c* and *d*.

The late type star JTH 826 has sufficient counts to obtain acceptable spectra in two observations (Obs. *a* and *f* of Table 1). Part of Obs. *f* a flare that could involve spectral variations. However, this flare interested only a small part ( $\approx 10\%$ ) of the observation, and the relatively poor statistic did not allow us to separately fit flaring and quiescent parts of the observation. The spectra in the two observation do not present evidence of spectral variability.

Finally, JTH 15509, a B2 star, is the optically brightest and hottest blue star of the cluster; suitable for a search for spectral variability. Dachs & Hummel (1996) give for this star an age of the order of one quarter of that estimated for the cluster ( $\sim 2.5 \times 10^7$  yr), suggesting that it is a blue straggler formed by mass transfer from a companion star in a close binary system. The X-ray emission observed in B stars is generally attributed to either intrinsic emission arising from shock heating of the surrounding medium by a high-velocity, radiatively driven wind or to the presence of an active, late-type companion (e.g. Dachs & Hummel 1996; Cassinelli et al. 1994). Recent results on early-type stars in the Orion Nebula (Stelzer et al. 2005)

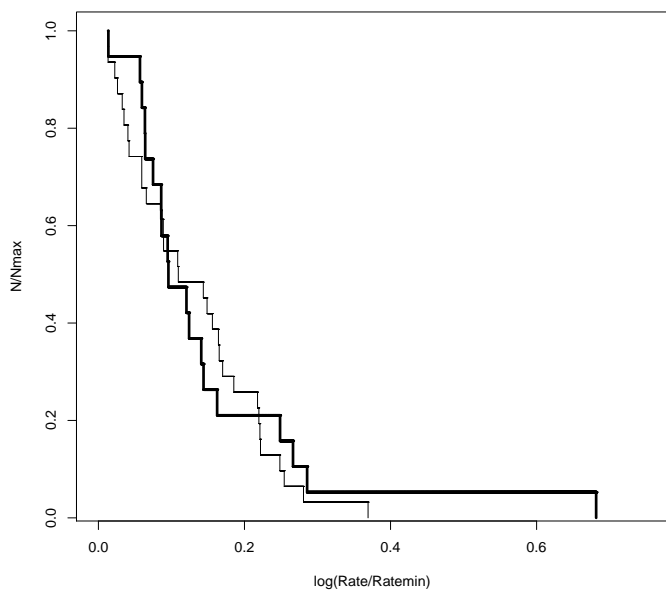


**Fig. 2.** The Time XAD for dF7-dK2 stars on short ( $\leq 1$  day, Obs. *a-b, d-e*, thin line) and long ( $\sim 17$  months, Obs. *c-f*, thick line) time scales.

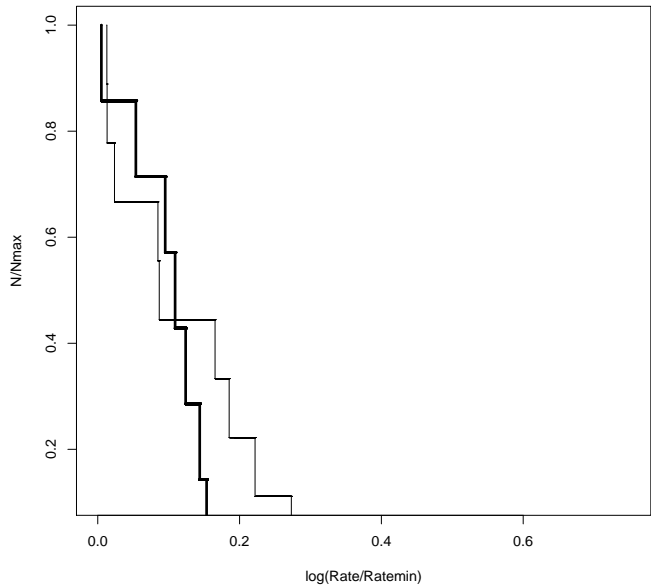


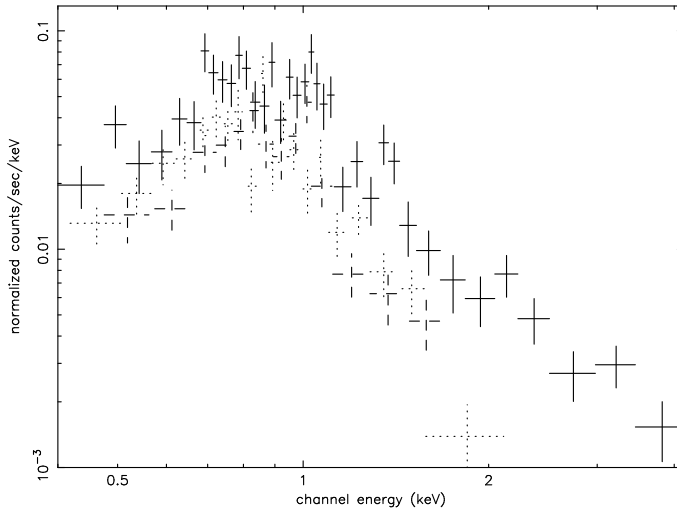
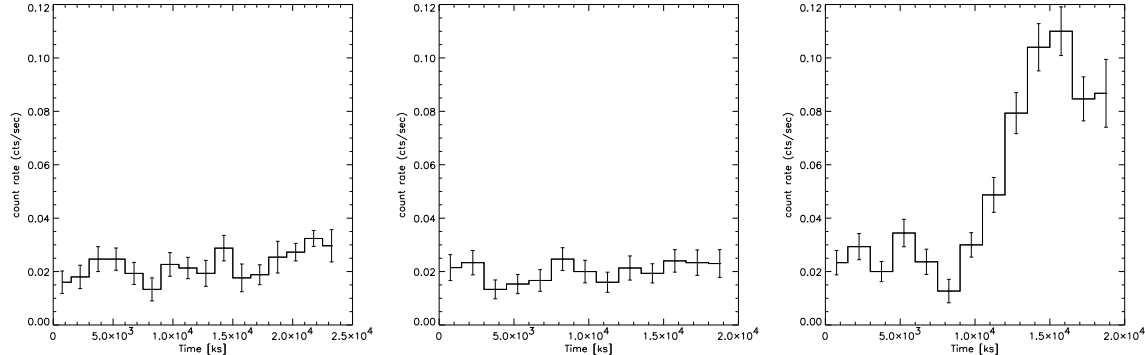
**Fig. 3.** As in Figure 2 for dK3-dM on short (thin line) and long (thick line) time scales.

hint that X-ray emission mechanism in hot stars is more complex than the simple wind-shock picture, suggesting in particular that magnetic phenomena may be important even in massive stars.

A simultaneous fit of four observations (Obs. *a, c, d, f* in Table 1) with a sum of two APEC models plus a photometric absorption provides the best fit to the data, as measured with an  $\chi^2$  test ( $\chi^2_\nu=1.3$  for 82 degrees of free-

**Table 5.** Stars for which spectral variability search was possible.

JTH	RA (J2000)	Dec (J2000)	V	B-V
826	07:58:43.392	-60:55:26.76	13.84	0.818
15510	07:58:50.352	-60:38:38.90	9.51	0.080
15509	07:58:50.616	-60:49:29.57	5.80	-0.090

**Fig. 7.** Spectra of JTH 15510 in the *c* (dotted lines), *d* (dashed lines) and *f* (solid lines) Obs. respectively.**Fig. 8.** From the left: light curves of JTH 15510 in the *c*, *d* and *f* Obs. respectively.

dom). Assuming under-solar abundances at 0.3 and  $N_H = 6 \times 10^{20} \text{ cm}^{-2}$ , we obtained temperatures of 0.91 keV and 3.29 keV, with a ratio of the emission measure of  $\text{EM}_{\text{hot}}/\text{EM}_{\text{cold}} \approx 7.49$ . No evidence of spectral variability is present.

## 5. Summary and conclusions

We analysed the variability of members of the open cluster NGC 2516 observed with XMM-Newton/EPIC. Using six XMM-Newton/EPIC observations, we explored X-ray variability on short ( $< 1$  day), medium (months), and long (years) time scales. We detected 303 distinct detections corresponding to 867 sources, and 474 of these sources were identified with 194 members of the cluster. Stars with spectral type ranging from B-type to M- were most detected.

Variability on short time scales is not very common among NGC 2516 members likely due to the limited statistics of our observations; the Kolmogorov-Smirnov test applied to all X-ray photon time series of detected cluster members shows that only a small fraction (12%) of the cluster members are variable at a confidence level greater than 99%, suggesting that the X-ray variability does not depend on stellar mass.

We computed the time distribution function of the X-ray amplitude variations for late-type stars in our sample. This distribution yields the fraction of time that a star spends with a flux higher, by a certain factor, than its minimum value. Our results show that the time XADs on the short and medium time scales of solar-like (dF7-dK2) stars are very alike. A similar result has been found for low-mass stars (dK3-dM), suggesting that, on the time scales we explored (from  $< 1$  day to 17 months), the am-

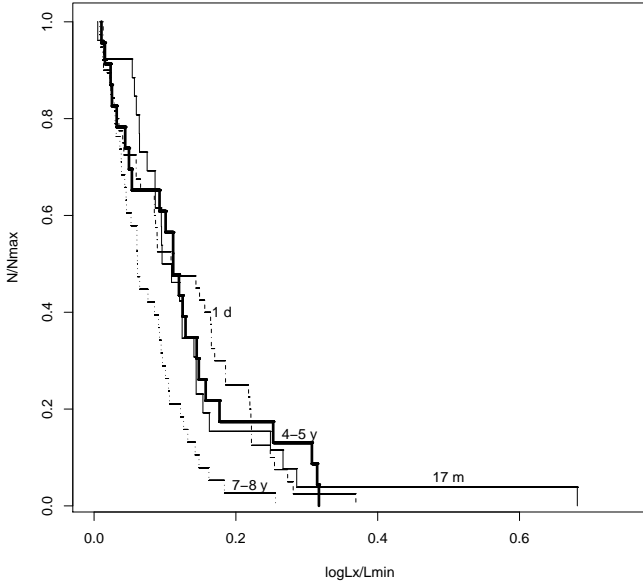


**Fig. 4.** The Time XADs for dF7-dM on 7-8 years (dotted line), on 4-5 years (thick line), on  $\sim$  17 months (thin solid line) and 1 day (dot-dashed line) time scales.

plitude of variability does not change with mass. Note that at ages higher than that of this cluster, solar-like stars are less variable than low mass stars (Marino et al. 2002). Comparing our data with the ROSAT/PSPC (on time scales of 7-8 yr) and ROSAT/HRI (on time scales of 4-5 yr) observations of late-type stars of the cluster, we find no evidence for long-term cyclic variability with amplitude similar to the solar one.

The comparison of time XADs for dF7-dK2 and dK3-dM NGC 2516 stars with the corresponding of the coeval Pleiades shows that the amplitude variations for the two samples are consistent. We searched for spectral variability in the cluster members for which more than one spectrum was available. We find evidence of spectral variability only in one star due to a flare in one observation.

*Acknowledgements.* This work is based on observations obtained by XMM-Newton, an ESA science mission with instruments and contributions directly funded by ESA Member States and the USA (NASA). We acknowledge financial support from MIUR and the anonymous referee.

## References

- Ambruster, C. W., Sciortino, S., & Golub, L. 1987, ApJS, 65, 273  
 Baliunas, S. L., Donahue, R. A., Soon, W. H., et al. 1995, ApJ, 438, 269  
 Barbera, M., Micela, G., Sciortino, S., Harnden, F. R., & Rosner, R. 1993, ApJ, 414, 846  
 Briggs, K. R. & Pye, J. P. 2003, MNRAS, 345, 714  
 Cassinelli, J. P., Cohen, D. H., Macfarlane, J. J., Sanders, W. T., & Welsh, B. Y. 1994, ApJ, 421, 705  
 Dachs, J. & Hummel, W. 1996, A&A, 312, 818  
 Damiani, F., Flaccomio, E., Micela, G., et al. 2003, ApJ, 588, 1009  
 Damiani, F., Maggio, A., Micela, G., & Sciortino, S. 1997a, ApJ, 483, 350  
 Damiani, F., Maggio, A., Micela, G., & Sciortino, S. 1997b, ApJ, 483, 370  
 Favata, F., Micela, G., Baliunas, S. L., et al. 2004, A&A, 418, L13  
 Franciosini, E., Randich, S., & Pallavicini, R. 2003, A&A,

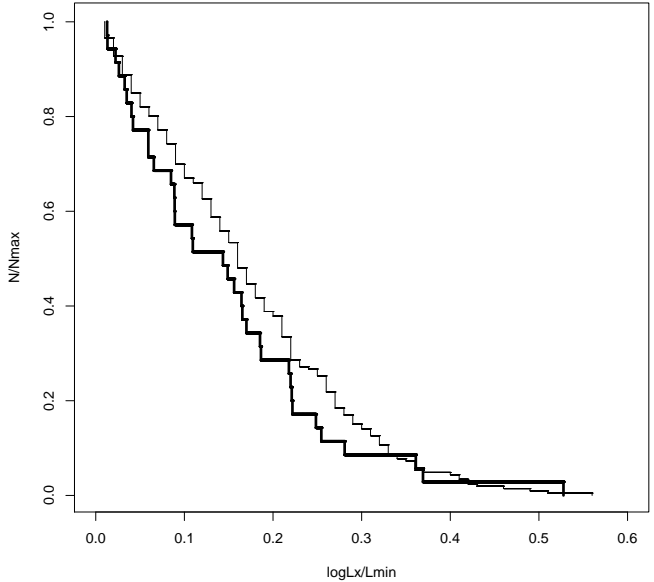


**Fig. 5.** The Time XAD for NGC 2516 (thick line) and Pleiades (thin line) dF7-dK2 stars.

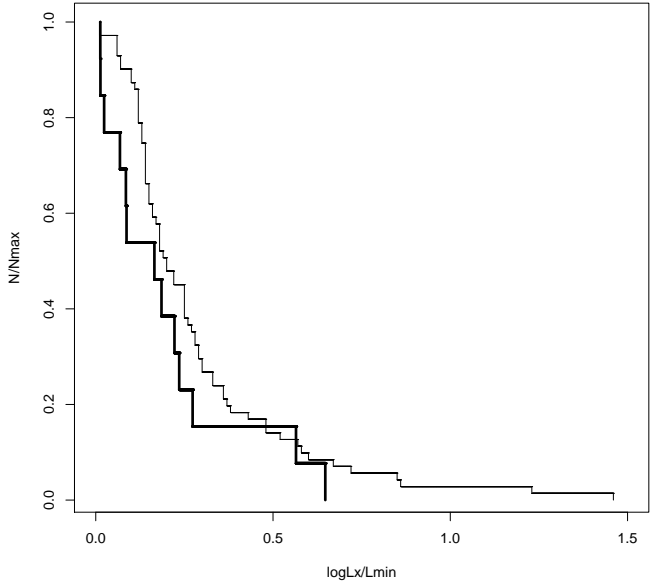


**Fig. 6.** As in Figure 5 for dK3-dM stars.

- 405, 551
- Gagné, M., Caillault, J., & Stauffer, J. R. 1995, ApJ, 450, 217
- Harnden, F. R., Adams, N. R., Damiani, F., et al. 2001, ApJ, 547, L141
- Hempelmann, A., Schmitt, J. H. M. M., Baliunas, S. L., & Donahue, R. A. 2003, A&A, 406, L39
- Jeffries, R. D., James, D. J., & Thurston, M. R. 1998, MNRAS, 300, 550
- Jeffries, R. D., Thurston, M. R., & Hambly, N. C. 2001, A&A, 375, 863
- Jeffries, R. D., Thurston, M. R., & Pye, J. P. 1997, MNRAS, 287, 350
- Kreplin, R. W. Dere, K. P., M., H. D., & Meekins, J. F. 1977, The solar output and its variations (Colorado University press), 187
- Maggio, A., Sciortino, S., Vaiana, G. S., et al. 1987, ApJ, 315, 687
- Marino, A., Micela, G., & Peres, G. 2000, A&A, 353, 177
- Marino, A., Micela, G., Peres, G., Pillitteri, I., & Sciortino, S. 2005, A&A, 430, 287
- Marino, A., Micela, G., Peres, G., & Sciortino, S. 2002, A&A, 383, 210
- Marino, A., Micela, G., Peres, G., & Sciortino, S. 2003a, A&A, 407, L63
- Marino, A., Micela, G., Peres, G., & Sciortino, S. 2003b, A&A, 406, 629
- Micela, G. & Marino, A. 2003, A&A, 404, 637
- Micela, G., Sciortino, S., Jeffries, R. D., Thurston, M. R., & Favata, F. 2000, A&A, 357, 909
- Micela, G., Sciortino, S., Kashyap, V., et al. 1996, ApJS, 102, 75
- Micela, G., Sciortino, S., Serio, S., et al. 1985, ApJ, 292, 172
- Micela, G., Sciortino, S., Vaiana, G. S., et al. 1990, ApJ, 348, 557
- Montmerle, T., Koch-Miramond, L., Falgarone, E., & Grindlay, J. E. 1983, ApJ, 269, 182
- Peres, G., Orlando, S., Reale, F., Rosner, R., & Hudson, H. 2000, ApJ, 528, 537
- Pillitteri, I., Micela, G., Damiani, F., & Sciortino, S. 2006, A&A, in press
- Pillitteri, I., Micela, G., Reale, F., & Sciortino, S. 2005, A&A, 430, 155
- Pillitteri, I., Micela, G., Sciortino, S., Damiani, F., & Harnden, F. R. 2004, A&A, 421, 175
- Pinsonneault, M. H., Stauffer, J., Soderblom, D. R., King, J. R., & Hanson, R. B. 1998, ApJ, 504, 170
- Randich, S., Schmitt, J. H. M. M., Prosser, C. F., & Stauffer, J. R. 1995, A&A, 300, 134
- Read, A. M. & Ponman, T. J. 2003, A&A, 409, 395
- Robichon, N., Arenou, F., Mermilliod, J.-C., & Turon, C. 1999, A&A, 345, 471
- Sciortino, S., Damiani, F., Favata, F., Flaccomio, E., & Micela, G. 2002, in ASP Conf. Ser. 277: Stellar Coronae in the Chandra and XMM-Newton Era, 389
- Stauffer, J. R., Caillault, J.-P., Gagne, M., Prosser, C. F., & Hartmann, L. W. 1994, ApJS, 91, 625
- Stelzer, B., Flaccomio, E., Montmerle, T., et al. 2005, ApJS, in press
- Stern, R. A., Schmitt, J. H. M. M., & Kahabka, P. T. 1995, ApJ, 448, 683
- Terndrup, D. M., Pinsonneault, M., Jeffries, R. D., et al. 2002, ApJ, 576, 950
- Vaiana, G. S., Cassinelli, J. P., Fabbiano, G., et al. 1981, ApJ, 245, 163
- Wilson, O. C. 1978, ApJ, 226, 379
- Wolk, S. J., Harnden, F. R., Murray, S. S., et al. 2004, ApJ, 606, 466